おわりに

ヒト ES/iPS 細胞から肝細胞への分化誘導において、使用する液性因子、低分子化合物、細胞外基質、共培養細胞など様々な培養条件が検討されてきた。本稿で紹介したように、肝分化に関連した転写因子を分化過程の細胞に遺伝子導入することによって、さらなる肝分化誘導効率の向上が可能になったが、ヒト ES/iPS 細胞から肝細胞への分化誘導は現在まさに研究開発途上の技術である。今後、分化誘導肝細胞を作製する技術がさらに向上し、よりヒト初代培養肝細胞に類似した機能を有した細胞が作製されることで、薬物の毒性評価系への応用をはじめとする創薬研究、さらには再生医療への応用に貢献することが期待される。

文　献

1) Greer, M. L., Barber, J., Eakins, J. and Kenna, J. G.: Cell based approaches for evaluation of drug-induced liver injury. Toxicology, 268, 125–131, 2010.
2) Li, A. P., Lu, C., Brent, J. A., Pham, C., Fackett, A., Ruegg, C. E. and Silber, P. M.: Cryopreserved human hepatocytes: characterization of drug-metabolizing enzyme activities and applications in higher throughput screening assays for hepatotoxicity, metabolic stability, and drug-drug interaction potential. Chem Biol Interact, 121, 17–35, 1999.
3) Gomez-Lechon, M. J., Donato, T., Jover, R., Rodriguez, C., Ponsoda, X., Glaise, D., Castell, J. V. and Guguen-Guillouzo, C.: Expression and induction of a large set of drug-metabolizing enzymes by the highly differentiated human hepatoma cell line BC2. Eur J Biochem, 268, 1448–1459, 2001.
4) Thomson, J. A., Itskovitz-Eldor, J., Shapiro, S. S., Waknitz, M. A., Swiergiel, J. J., Marshall, V. S. and Jones, J. M.: Embryonic stem cell lines derived from human blastocysts. Science, 282, 1145–1147, 1998.
5) Takahashi, K., Tanabe, K., Ohnuki, M., Narita, M., Ichisaka, T., Tomoda, K. and Yamanaka, S.: Induction of pluripotent stem cells from adult human fibroblasts by defined factors. Cell, 131, 861–872, 2007.
6) Basma, H., Soto-Gutierrez, A., Yannam, G. R., Liu, L., Ito, R., Yamamoto, T., Ellis, E., Carson, S. D., et al.: Differentiation and transplantation of human embryonic stem cell-derived hepatocytes. Gastroenterology, 136, 990–999, 2009.
7) Asahina, K., Fujimori, H., Shimizu-Saito, K., Kumashiro, Y., Okamura, K., Tanaka, Y., Teramoto, K., Arii, S., et al.: Expression of the liver-specific gene Cyp7a1 reveals hepatic differentiation in embryoid bodies derived from mouse embryonic stem cells. Genes Cells, 9, 1297–1308, 2004.
8) Duan, Y., Ma, X., Zou, W., Wang, C., Bahbahan, I. S., Ahuja, T. P., Tolstikov, V. and Zern, M. A.: Differentiation and characterization of metabolically functioning hepatocytes from human embryonic stem cells. Stem Cells, 28, 674–686, 2010.
9) Cai, J., Zhao, Y., Liu, Y., Ye, F., Song, Z., Qin, H., Meng, S., Chen, Y., et al.: Directed differentiation of human embryonic stem cells into functional hepatic cells. Hepatology, 45, 1229–1239, 2007.
10) Takayama, K., Inamura, M., Kawabata, K., Katayama, K., Higuchi, M., Tashiro, K., Nonaka, A., Sakurai, F., et al.: Efficient Generation of Functional Hepatocytes From Human Embryonic Stem Cells and Induced Pluripotent Stem Cells by HNF4alpha Transduction. Mol Ther, 20, 127–137, 2012.
11) Usui, T., Mise, M., Hashizume, T., Yabuki, M. and Komuro, S.: Evaluation of the potential for drug-induced liver injury based on in vitro covalent binding to human liver proteins. Drug Metab Dispos, 37, 2383–2392, 2009.
12) Si-Tayeb, K., Noto, F. K., Nagaoka, M., Li, J., Battle, M. A., Duris, C., North, P. E., Dalton, S., et al.: Highly efficient generation of human hepatocyte-like cells from induced pluripotent stem cells. Hepatology, 51, 297–305, 2010.
13) Agarwal, S., Holton, K. L. and Lanza, R.: Efficient differentiation of functional hepatocytes from human embryonic stem cells. Stem Cells, 26, 1117–1127, 2008.
14) Takayama, K., Inamura, M., Kawabata, K., Tashiro, K., Katayama, K., Sakurai, F., Hayakawa, T., Furue, M. K., et al.: Efficient and directive generation of two distinct endoderm lineages from human ESCs and iPSCs by differentiation stage-specific SOX17 transduction. PLoS One, 6, e21780, 2011.
15) Inamura, M., Kawabata, K., Takayama, K., Tashiro, K., Sakurai, F., Katayama, K., Toyoda, M., Akutsu, H., et al.: Efficient generation of hepatoblasts from human ES cells and iPS cells by transient overexpression of homeobox gene HEX. Mol Ther, 19, 400–407, 2011.
16) Takayama, K., Inamura, M., Kawabata, K., Sugawara, M., Kikuchi, K., Higuchi, M., Nagamoto, Y.,

Watanabe, H., et al.: Generation of metabolically functioning hepatocytes from human pluripotent stem cells by FOXA2 and HNF1alpha transduction. J Hepatol, 57, 628–636, 2012.
17) Takayama, K., Kawabata, K., Nagamoto, Y., Kishimoto, K., Tashiro, K., Sakurai, F., Tachibana, M., Kanda, K., et al.: 3D spheroid culture of hESC/hiPSC-derived hepatocyte-like cells for drug toxicity testing. Biomaterials, 34, 1781-9, 2013.
18) Labbe, G., Pessayre, D. and Fromenty, B.: Drug-induced liver injury through mitochondrial dysfunction: mechanisms and detection during preclinical safety studies. Fundam Clin Pharmacol, 22, 335–353, 2008.
19) Rachek, L. I., Yuzefovych, L. V., Ledoux, S. P., Julie, N. L. and Wilson, G. L.: Troglitazone, but not rosiglitazone, damages mitochondrial DNA and induces mitochondrial dysfunction and cell death in human hepatocytes. Toxicol Appl Pharmacol, 240, 348–354, 2009.
20) Lawless, M. W., Mankan, A. K., Gray, S. G. and Norris, S.: Endoplasmic reticulum stress—a double edged sword for Z alpha-1 antitrypsin deficiency hepatoxicity. Int J Biochem Cell Biol, 40, 1403–1414, 2008.
(Accepted 1 April 2013)

Generation of hepatocyte-like cells from human pluripotent stem cells for drug screening

Kazuo Takayama[1,2], Kenji Kawabata[2] and Hiroyuki Mizuguchi[1-3]

[1] Laboratory of Biochemistry and Molecular Biology, Graduate School of Pharmaceutical Sciences, Osaka University, Osaka 565–0871, Japan
[2] Laboratory of Stem Cell Regulation, National Institute of Biomedical Innovation, Osaka 567–0085, Japan
[3] The Center for Advanced Medical Engineering and Informatics, Osaka University, Osaka 565–0871, Japan

Abstract

Human embryonic stem (ES) cell and induced pluripotent stem (iPS) cell have ability to differentiate into all body cells, including hepatocytes. Hepatocyte-like cells generated from human ES/iPS cells are expected to be utilized in medical application such as drug screening. However, the existing protocols for hepatic differentiation of pluripotent stem cells are not enough efficient. To promote hepatic differentiation, we developed an efficient method to differentiate hepatocyte-like cells from human ES/iPS cells by overexpression of the hepatocyte-related genes. In this review, we will introduce the present status and feature view of the hepatic differentiation from human ES/iPS cells.

Key words: hepatocytes, human ES cells, human iPS cells, drug screening

© 2014. Published by The Company of Biologists Ltd | Development (2014) 141, 91-100 doi:10.1242/dev.103168

RESEARCH ARTICLE

STEM CELLS AND REGENERATION

CCAAT/enhancer binding protein-mediated regulation of TGFβ receptor 2 expression determines the hepatoblast fate decision

Kazuo Takayama[1,2,3], Kenji Kawabata[4], Yasuhito Nagamoto[1,2], Mitsuru Inamura[1], Kazuo Ohashi[5], Hiroko Okuno[1], Tomoko Yamaguchi[4], Katsuhisa Tashiro[4], Fuminori Sakurai[1], Takao Hayakawa[6], Teruo Okano[5], Miho Kusada Furue[7,8] and Hiroyuki Mizuguchi[1,2,3,9,*]

ABSTRACT

Human embryonic stem cells (hESCs) and their derivatives are expected to be used in drug discovery, regenerative medicine and the study of human embryogenesis. Because hepatocyte differentiation from hESCs has the potential to recapitulate human liver development *in vivo*, we employed this differentiation method to investigate the molecular mechanisms underlying human hepatocyte differentiation. A previous study has shown that a gradient of transforming growth factor beta (TGFβ) signaling is required to segregate hepatocyte and cholangiocyte lineages from hepatoblasts. Although CCAAT/enhancer binding proteins (c/EBPs) are known to be important transcription factors in liver development, the relationship between TGFβ signaling and c/EBP-mediated transcriptional regulation in the hepatoblast fate decision is not well known. To clarify this relationship, we examined whether c/EBPs could determine the hepatoblast fate decision via regulation of TGFβ receptor 2 (TGFBR2) expression in the hepatoblast-like cells differentiated from hESCs. We found that *TGFBR2* promoter activity was negatively regulated by c/EBPα and positively regulated by c/EBPβ. Moreover, c/EBPα overexpression could promote hepatocyte differentiation by suppressing TGFBR2 expression, whereas c/EBPβ overexpression could promote cholangiocyte differentiation by enhancing TGFBR2 expression. Our findings demonstrated that c/EBPα and c/EBPβ determine the lineage commitment of hepatoblasts by negatively and positively regulating the expression of a common target gene, *TGFBR2*, respectively.

KEY WORDS: Hepatoblasts, c/EBP, CEBP, Human ESCs

INTRODUCTION

Many animal models, such as chick, *Xenopus*, zebrafish and mouse, have been used to investigate the molecular mechanisms of liver development. Because many functions of the key molecules in liver development are conserved in these species, studies on liver development in these animals can be highly informative with respect that in humans. However, some functions of important molecules in liver development might differ between human and other species. Although analysis using genetically modified mice has been successfully performed, it is not of course possible to perform genetic experiments to elucidate molecular mechanisms of liver development in human. Pluripotent stem cells, such as human embryonic stem cells (hESCs), are expected to overcome some of these problems in the study of human embryogenesis, including liver development, because the gene expression profiles of this model are similar to those in normal liver development (Agarwal et al., 2008; DeLaForest et al., 2011).

During liver development, hepatoblasts differentiate into hepatocytes and cholangiocytes. A previous study has shown that a high concentration of transforming growth factor beta (TGFβ) could give rise to cholangiocyte differentiation from hepatoblasts (Clotman et al., 2005). To transmit the TGFβ signaling, TGFβ receptor 2 (TGFBR2) has to be stimulated by TGFβ1, TGFβ2 or TGFβ3 (Kitisin et al., 2007). TGFβ binding to the extracellular domain of TGFBR2 induces a conformational change, resulting in the phosphorylation and activation of TGFBR1. TGFBR1 phosphorylates SMAD2 or SMAD3, which binds to SMAD4, and then the SMAD complexes move into the nucleus and function as transcription factors to express various kinds of differentiation-related genes (Kitisin et al., 2007). Although the function of TGFBR2 in regeneration of the adult liver has been thoroughly examined (Oe et al., 2004), the function of TGFBR2 in the hepatoblast fate decision has not been elucidated.

CCAAT/enhancer binding protein (c/EBP) transcription factors play decisive roles in the differentiation of various cell types, including hepatocytes (Tomizawa et al., 1998; Yamasaki et al., 2006). The analysis of *c/EBPα* (*Cebpa*) knockout mice has shown that many abnormal pseudoglandular structures, which co-express antigens specific for both hepatocytes and cholangiocytes, are present in the liver parenchyma (Tomizawa et al., 1998). These data demonstrated that c/EBPα plays an important role in hepatocyte differentiation. It is also known that the suppression of c/EBPα expression in periportal hepatoblasts stimulates cholangiocyte differentiation (Yamasaki et al., 2006). Although the function of c/EBPα in liver development is well known, the relationship between TGFβ signaling and c/EBPα-mediated transcriptional regulation in the hepatoblast fate decision is poorly understood. c/EBPβ is also known to be an important factor for liver function (Chen et al., 2000), although the function of c/EBPβ in the cell fate decision of hepatoblasts is not well known. c/EBPα and c/EBPβ bind to the same DNA binding site. However, the promoter activity of hepatocyte-specific genes, such as those encoding hepatocyte nuclear factor 6 (HNF6, also known as ONECUT1) and UGT2B1,

[1]Laboratory of Biochemistry and Molecular Biology, Graduate School of Pharmaceutical Sciences, Osaka University, Osaka 565-0871, Japan. [2]Laboratory of Hepatocyte Differentiation, National Institute of Biomedical Innovation, Osaka 567-0085, Japan. [3]iPS Cell-based Research Project on Hepatic Toxicity and Metabolism, Graduate School of Pharmaceutical Sciences, Osaka University, Osaka 565-0871, Japan. [4]Laboratory of Stem Cell Regulation, National Institute of Biomedical Innovation, Osaka 567-0085, Japan. [5]Institute of Advanced Biomedical Engineering and Science, Tokyo Women's Medical University, Tokyo 162-8666, Japan. [6]Pharmaceutical Research and Technology Institute, Kinki University, Osaka 577-8502, Japan. [7]Laboratory of Embryonic Stem Cell Cultures, Department of Disease Bioresources Research, National Institute of Biomedical Innovation, Osaka 567-0085, Japan. [8]Department of Embryonic Stem Cell Research, Field of Stem Cell Research, Institute for Frontier Medical Sciences, Kyoto University, Kyoto 606-8507, Japan. [9]The Center for Advanced Medical Engineering and Informatics, Osaka University, Osaka 565-0871, Japan.

*Author for correspondence (mizuguch@phs.osaka-u.ac.jp)

Received 27 August 2013; Accepted 3 October 2013

is positively regulated by c/EBPα but not c/EBPβ (Hansen et al., 1998; Plumb-Rudewiez et al., 2004), suggesting that the functions of c/EBPα and c/EBPβ in the hepatoblast fate decision might be different.

In the present study, we first examined the function of TGFBR2 in the hepatoblast fate decision using hESC-derived hepatoblast-like cells, which have the ability to self-replicate, differentiate into both hepatocyte and cholangiocyte lineages, and repopulate the liver of carbon tetrachloride (CCl_4)-treated immunodeficient mice. *In vitro* gain- and loss-of-function analyses and *in vivo* transplantation analysis were performed. Next, we investigated how TGFBR2 expression is regulated in the hepatoblast fate decision. Finally, we examined whether our findings could be reproduced in delta-like 1 homolog (Dlk1)-positive hepatoblasts obtained from the liver of E13.5 mice. To the best of our knowledge, this study provides the first evidence of c/EBP-mediated regulation of TGFBR2 expression in the human hepatoblast fate decision.

RESULTS

Hepatoblast-like cells are generated from hESCs

First, we investigated whether the hepatoblast-like cells (HBCs), which were differentiated from hESCs as described in supplementary material Fig. S1A, have similar characteristics to human hepatoblasts. We recently found that hESC-derived HBCs could be purified and maintained on human laminin 111 (LN111)-coated dishes (Takayama et al., 2013). The long-term cultured HBC population (HBCs passaged more than three times were used in this study) were nearly homogeneous and expressed human hepatoblast markers such as alpha-fetoprotein (AFP), albumin (ALB), cytokeratin 19 (CK19, also known as KRT19) and EPCAM (Schmelzer et al., 2007) (supplementary material Fig. S1B). In addition, most of the colonies observed on human LN111-coated plates were ALB and CK19 double positive, although a few colonies were ALB single positive, CK19 single positive, or ALB and CK19 double negative (supplementary material Fig. S1C). To examine the hepatocyte differentiation capacity of the HBCs *in vivo*, these cells were transplanted into CCl_4-treated immunodeficient mice. The hepatocyte functionality of the transplanted cells was assessed by measuring secreted human ALB levels in the recipient mice (supplementary material Fig. S1D). Human ALB serum was detected in the mice that were transplanted with the HBCs, but not in the control mice. These results demonstrated that the HBCs generated from hESCs have similar characteristics to human hepatoblasts and would therefore provide a valuable tool to investigate the mechanisms of human liver development. In the present study, HBCs generated from hESCs were used to elucidate the mechanisms of the hepatoblast fate decision.

TGFBR2 expression is decreased in hepatocyte differentiation but increased in cholangiocyte differentiation

The HBCs used in this study have the ability to differentiate into both hepatocyte-like cells [cytochrome P450 3A4 (CYP3A4) positive; Fig. 1B] and cholangiocyte-like cells (CK19 positive; Fig. 1C) (the protocols are described in Fig. 1A). Because the expression pattern of TGFBR2 during differentiation from hepatoblasts is not well known, we examined it in hepatocyte and cholangiocyte differentiation from HBCs. *TGFBR2* was downregulated during hepatocyte differentiation from HBCs (Fig. 1D), but upregulated in cholangiocyte differentiation from HBCs (Fig. 1E). After the HBCs were cultured on Matrigel, the cells were fractionated into three populations according to the level of TGFBR2 expression (TGFBR2-negative, -lo or -hi; Fig. 1F). The HBC-derived TGFBR2-lo cells strongly expressed *αAT* and *CYP3A4* (hepatocyte markers), whereas the HBC-derived TGFBR2-hi cells strongly expressed *SOX9* and integrin β4 (*ITGB4*) (cholangiocyte markers). These data suggest that the TGFBR2 expression level is decreased in hepatic differentiation, but increased in biliary differentiation of the HBCs.

The cell fate decision of HBCs is regulated by TGFβ signals

To examine the function of TGFβ1, β2 and β3 (all of which are ligands of TGFBR2) in the hepatoblast fate decision, HBCs were cultured in medium containing TGFβ1, β2 or β3 (Fig. 2A,B). The expression levels of cholangiocyte marker genes were upregulated by addition of TGFβ1 or TGFβ2, but not TGFβ3 (Fig. 2A), whereas those of hepatocyte markers were downregulated by addition of TGFβ1 or TGFβ2 (Fig. 2B). To ascertain that TGFBR2 is also important in the hepatoblast fate decision, HBCs were cultured in medium containing SB-431542, which inhibits TGFβ signaling (Fig. 2C,D). Hepatocyte marker genes were upregulated by inhibition of TGFβ signaling (Fig. 2C), whereas cholangiocyte markers were downregulated (Fig. 2D). To confirm the function of TGFβ1, β2 and β3 in the hepatoblast fate decision, colony assays of the HBCs were performed in the presence or absence of TGFβ1, β2 or β3 (Fig. 2E). The number of CK19 single-positive colonies was significantly increased in TGFβ1- or β2-treated HBCs. By contrast, the number of ALB and CK19 double-positive colonies was reduced in TGFβ1-, β2- or β3-treated HBCs. These data indicated that TGFβ1 and β2 positively regulate the biliary differentiation of HBCs. Taken together, the findings suggested that TGFBR2 might be a key molecule in the regulation of hepato-bilary lineage segregation.

TGFBR2 plays an important role in the cell fate decision of HBCs

To examine whether TGFBR2 plays an important role in the hepatoblast fate decision, *in vitro* gain- and loss-of-function analysis of TGFBR2 was performed in the HBCs. We used siRNA in knockdown experiments (supplementary material Fig. S2) during HBC differentiation on Matrigel. Whereas TGFBR2-suppressing siRNA (si-TGFBR2) transfection upregulated the expression of hepatocyte markers, it downregulated cholangiocyte markers (Fig. 3A). si-TGFBR2 transfection increased the percentage of asialoglycoprotein receptor 1 (ASGR1)-positive hepatocyte-like cells (Fig. 3B). By contrast, it decreased the percentage of aquaporin 1 (AQP1)-positive cholangiocyte-like cells. These results suggest that TGFBR2 knockdown promotes hepatocyte differentiation, whereas it inhibits cholangiocyte differentiation. Next, we used Ad vector to perform efficient transduction into the HBCs (supplementary material Fig. S3) and ascertained *TGFBR2* gene expression in TGFBR2-expressing Ad vector (Ad-TGFBR2)-transduced cells (supplementary material Fig. S4). Ad-TGFBR2 transduction downregulated the expression of hepatocyte markers, whereas it upregulated cholangiocyte markers (Fig. 3C). Ad-TGFBR2 transduction decreased the percentage of ASGR1-positive hepatocyte-like cells but increased the percentage of AQP1-positive cholangiocyte-like cells (Fig. 3D). These results suggest that TGFBR2 overexpression inhibits hepatocyte differentiation, whereas it promotes cholangiocyte differentiation. Taken together, these results suggest that TGFBR2 plays an important role in deciding the differentiation lineage of HBCs.

To investigate whether hepatoblasts would undergo differentiation in a TGFBR2-associated manner *in vivo*, HBCs transfected/transduced with si-control, si-TGFBR2, Ad-LacZ or Ad-

Development (2014) doi:10.1242/dev.103168

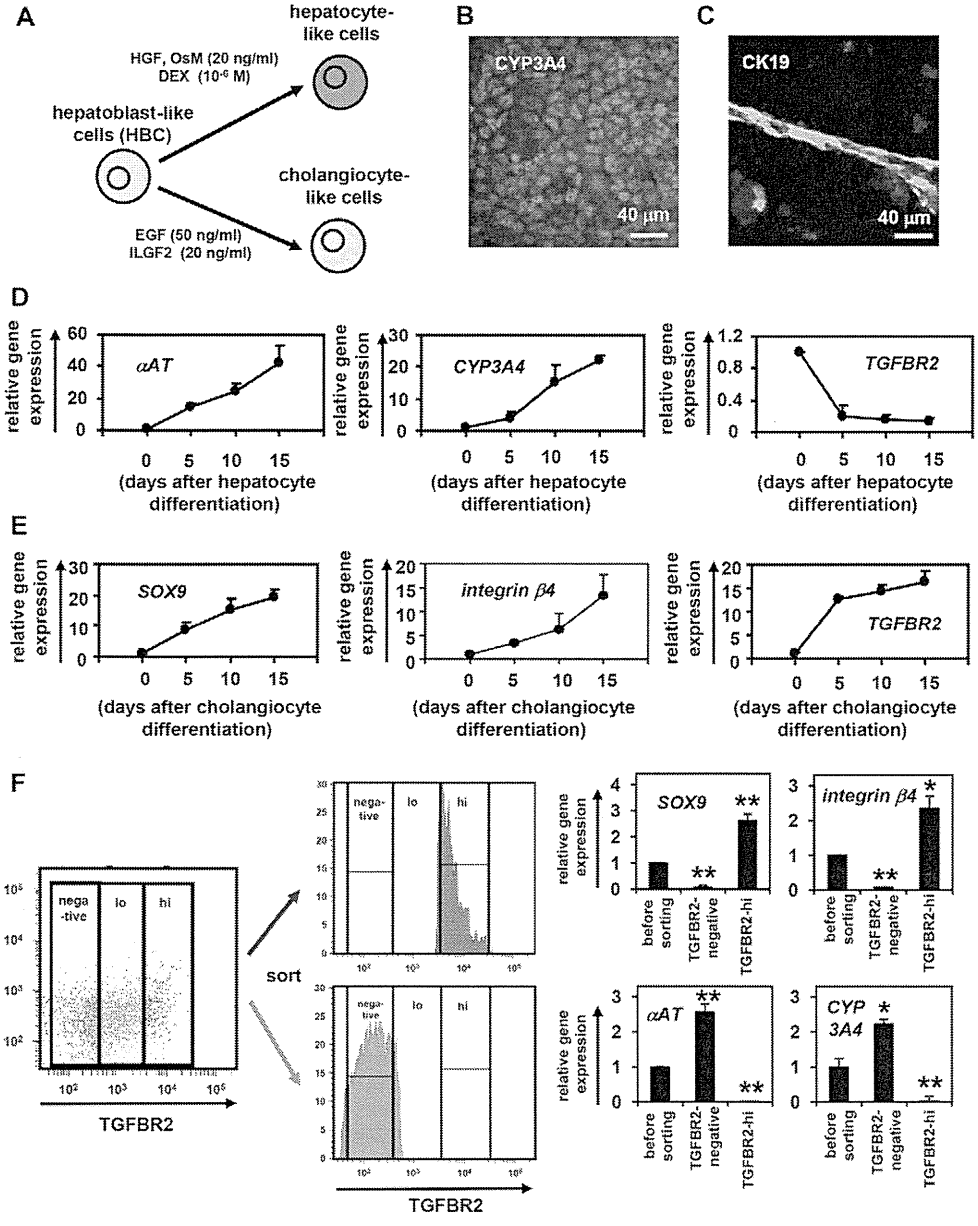

Fig. 1. HBCs can differentiate into both hepatocyte and cholangiocyte lineages. (A) The strategy for hepatocyte and cholangiocyte differentiation from HBCs. (B,C) The HBC-derived hepatocyte-like cells or cholangiocyte-like cells were subjected to immunostaining with anti-CYP3A4 (red, B) or anti-CK19 (green, C) antibodies, respectively. (D,E) Temporal gene expression levels of hepatocyte markers (*αAT* and *CYP3A4*) (D) or cholangiocyte markers (*SOX9* and integrin β4) (E) during hepatocyte or cholangiocyte differentiation as measured by real-time RT-PCR. The temporal gene expression of *TGFBR2* was also examined. The gene expression levels in HBCs were taken as 1.0. (F) HBCs were cultured on Matrigel for 5 days, and then the expression level of TGFBR2 was examined by FACS analysis. TGFBR2-negative, -lo and -hi populations were collected and real-time RT-PCR analysis was performed to measure the expression levels of hepatocyte markers (*αAT* and *CYP3A4*) and cholangiocyte markers (*SOX9* and integrin β4). **P*<0.05, ***P*<0.01 (compared with 'before sorting'). Error bars indicate s.d. Statistical analysis was performed using the unpaired two-tailed Student's *t*-test (n=3).

TGFBR2 were transplanted into CCl_4-treated immunodeficient mice (Fig. 3E,F). Although some of the si-control-transfected or Ad-LacZ-transduced HBCs remained as HBCs (HNF4α and CK19 double positive), most of them showed *in vitro* differentiation toward hepatocyte-like cells (HNF4α single positive) (Fig. 3E, top row). By contrast, Ad-TGFBR2-transduced HBCs were predominantly committed to cholangiocyte-like cells (CK19 single positive) and si-TGFBR2-transfected HBCs were predominantly committed to hepatocyte-like cells (HNF4α single positive) (Fig. 3E, bottom row). Ad-TGFBR2 transduction decreased the percentage of HNF4α-positive hepatocyte-like cells, whereas it increased the percentage of CK19-positive cholangiocyte-like cells (supplementary material Fig. S5). The hepatocyte functionality of the *in vivo* differentiated HBCs was assessed by measuring secreted human ALB levels in the recipient mice (Fig. 3F). Mice that were transplanted with Ad-TGFBR2-transduced HBCs showed lower human ALB serum levels than those transplanted with Ad-LacZ-transduced HBCs, and the mice that were transplanted with si-TGFBR2-transfected HBCs showed higher human ALB serum levels than those transplanted with si-control-transfected HBCs. These data suggest that cholangiocyte or hepatocyte differentiation was promoted by TGFBR2 overexpression or knockdown, respectively. Thus, based on these data from *in vitro* and *in vivo* experiments, TGFBR2 plays an important role in deciding the differentiation lineage of HBCs.

TGFBR2 promoter activity and expression are negatively regulated by c/EBPα and positively regulated by c/EBPβ

A previous study has shown that TGFBR2 expression is upregulated in *Hnf6* knockout mice (Clotman et al., 2005), although we confirmed by ChIP assay that HNF6 does not bind to the *TGFBR2* promoter region (data not shown). Because c/EBPα is important in the hepatoblast fate decision (Suzuki et al., 2003), we expected that c/EBPs might directly regulate TGFBR2 expression. The *TGFBR2* promoter region was analyzed to examine whether TGFBR2 expression is regulated by c/EBPs. Some c/EBP binding sites (supplementary material Fig. S6) were predicted by rVista 2.0 (http://rvista.dcode.org/) (Fig. 4A). By performing a ChIP assay, one

Development (2014) doi:10.1242/dev.103168

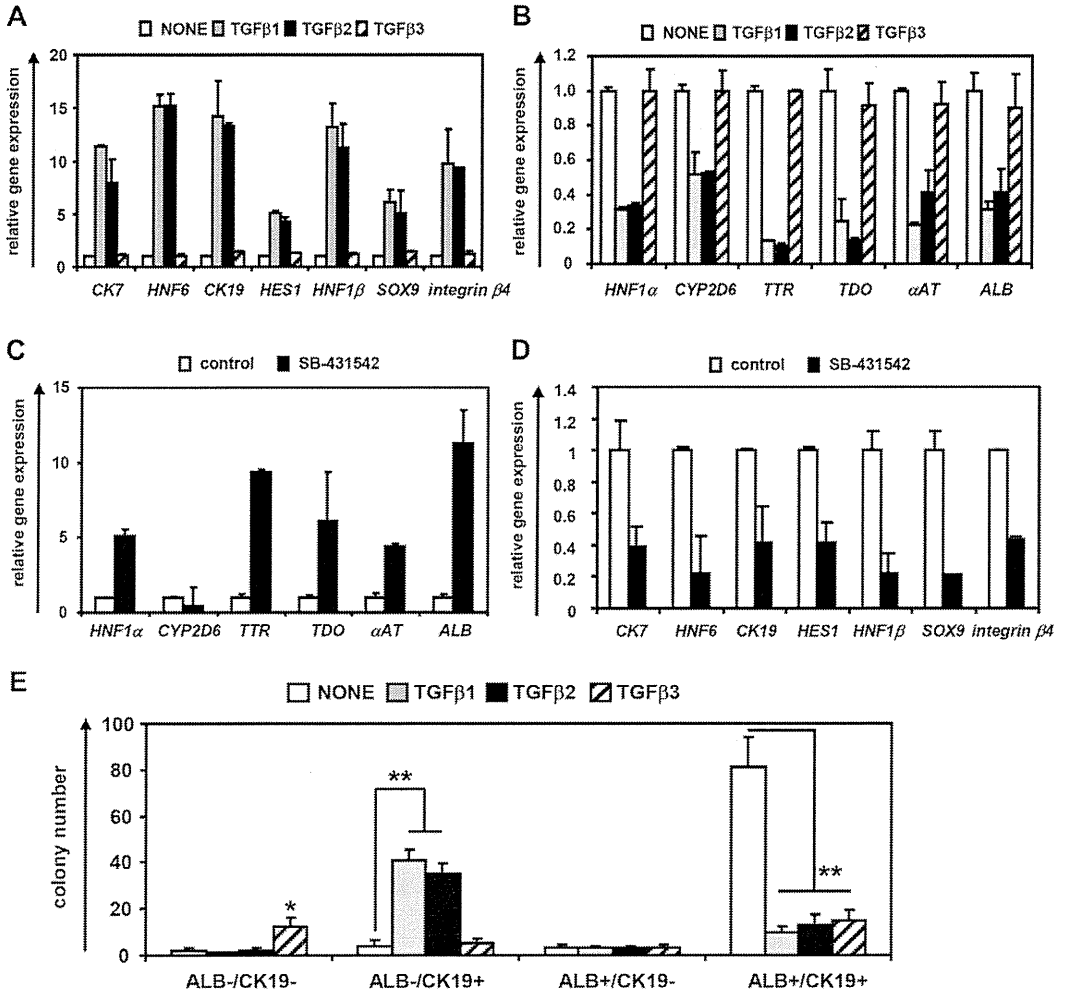

Fig. 2. Hepatocyte and cholangiocyte differentiation from HBCs is regulated by TGFβ signaling. (A,B) HBCs were cultured in differentiation hESF-DIF medium containing 10 ng/ml TGFβ1, TGFβ2 or TGFβ3 for 10 days. The expression levels of cholangiocyte (A) and hepatocyte (B) marker genes were measured by real-time RT-PCR. On the *y*-axis, the gene expression level of cholangiocyte markers in untreated cells (NONE) was taken as 1.0. (C,D) HBCs were cultured in differentiation hESF-DIF medium containing SB-431542 (10 μM) for 10 days. Control cells were treated with solvent only (0.1% DMSO). Expression levels of hepatocyte (C) and cholangiocyte (D) marker genes were measured by real-time RT-PCR. On the *y*-axis, the gene expression level of hepatocyte markers in untreated cells (control) was taken as 1.0. (E) HBC colony formation assay in the presence or absence of 10 ng/ml TGFβ1, TGFβ2 or TGFβ3. HBCs were plated at 200 cells/cm^2 on human LN111-coated dishes. The colonies were separated into four groups based on the expression of ALB and CK19: double-negative, ALB negative and CK19 positive, ALB positive and CK19 negative, and double positive. The numbers represent wells in which the colony was observed in three 96-well plates (total 288 wells). Five days after plating, the cells were fixed with 4% PFA and used for double immunostaining. **P*<0.05, ***P*<0.01 (compared with NONE). Error bars indicate s.d. Statistical analysis was performed using the unpaired two-tailed Student's *t*-test (*n*=3).

c/EBP binding site was found in the *TGFBR2* promoter region (Fig. 4B). A reporter assay of the *TGFBR2* promoter region showed that c/EBPβ activates *TGFBR2* promoter activity, whereas c/EBPα inhibits it (Fig. 4C). In addition, *TGFBR2* expression was downregulated by Ad-c/EBPα transduction, whereas *TGFBR2* was upregulated by Ad-c/EBPβ transduction in HepG2 cells (TGFBR2 positive) (Fig. 4D). We ascertained the expression of *c/EBPα* or *c/EBPβ* (*CEBPA* or *CEBPB* – Human Gene Nomenclature Committee) in the Ad-c/EBPα- or Ad-c/EBPβ-transduced cells, respectively (supplementary material Fig. S4). These results demonstrated that the promoter activity and expression of *TGFBR2* were directly regulated by both c/EBPα and c/EBPβ.

c/EBPs determine the cell fate decision of HBCs via regulation of TGFBR2 expression

To elucidate the relationship between TGFBR2 and c/EBPs (c/EBPα and c/EBPβ) in the hepatoblast fate decision, we first examined the temporal gene expression patterns of *TGFBR2*, *c/EBPα* and *c/EBPβ* in hepatocyte and cholangiocyte differentiation. During hepatocyte differentiation, *TGFBR2* expression was downregulated, whereas *c/EBPα* was upregulated (supplementary material Fig. S7A, top). During cholangiocyte differentiation, *c/EBPα* was downregulated, whereas *TGFBR2* and *c/EBPβ* were upregulated (supplementary material Fig. S7A, bottom). In addition, the ratio of *c/EBPα* to *c/EBPβ* was significantly increased in hepatocyte differentiation, but significantly reduced in cholangiocyte differentiation (supplementary material Fig. S7B). High-level expression of *c/EBPα* was detected in TGFBR2-negative cells, but not in TGFBR2-hi cells (supplementary material Fig. S7C). By contrast, high-level expression of *c/EBPβ* was detected in TGFBR2-hi cells, but not in TGFBR2-negative cells. These results suggest that TGFBR2 is negatively regulated by c/EBPα and positively regulated by c/EBPβ in the differentiation model from HBCs as well as in the HepG2 cell line (Fig. 4).

Development (2014) doi:10.1242/dev.103168

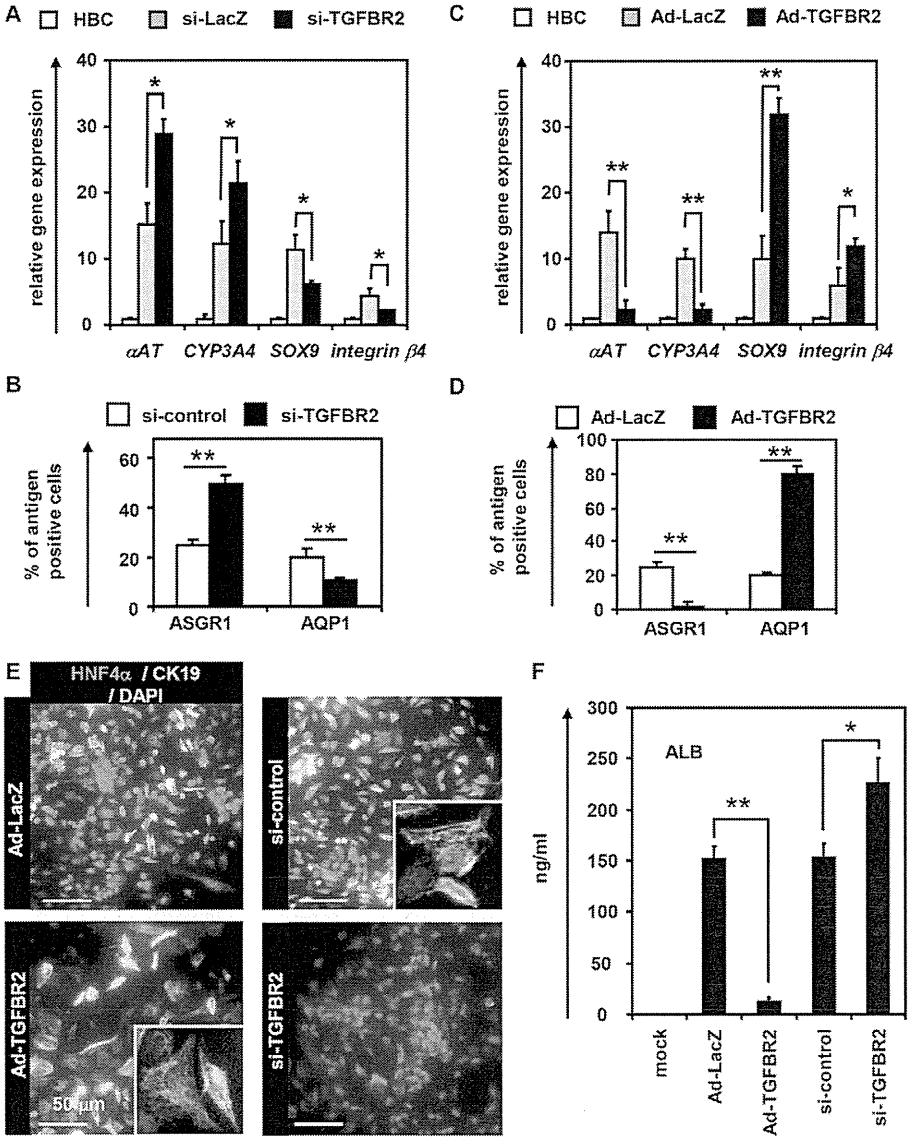

Fig. 3. TGFBR2 regulates bi-directional differentiation of HBCs. (A) HBCs were transfected with 50 nM control siRNA (si-control) or TGFBR2-suppressing siRNA (si-TGFBR2) and cultured in differentiation hESF-DIF medium for 10 days. The expression levels of hepatocyte (*αAT* and *CYP3A4*) or cholangiocyte (*SOX9* and integrin β4) markers were measured by real-time RT-PCR. On the *y*-axis, the gene expression level in HBCs was taken as 1.0. (B) On day 10 after siRNA transfection, the efficiency of hepatocyte or cholangiocyte differentiation was measured by estimating the percentage of ASGR1-positive or AQP1-positive cells, respectively, by FACS analysis. (C) HBCs were transduced with 3000 VPs/cell of Ad-LacZ or Ad-TGFBR2 for 1.5 hours and cultured in differentiation hESF-DIF medium for 10 days. Expression levels of hepatocyte or cholangiocyte marker genes were measured by real-time RT-PCR. On the *y*-axis, gene expression levels in the HBCs was taken as 1.0. (D) On day 10 after Ad vector transduction, the efficiency of hepatocyte or cholangiocyte differentiation was measured by estimating the percentage of ASGR1-positive or AQP1-positive cells, respectively, by FACS analysis. (E,F) The si-control, si-TGFBR2, Ad-LacZ- or Ad-TGFBR2-transfected/transduced HBCs (1.0×10^6 cells) were transplanted into CCl_4-treated (2 mg/kg) *Rag2/Il2rg* double-knockout mice by intrasplenic injection. (E) Expression of human HNF4α (red) and CK19 (green) was examined by double immunohistochemistry 2 weeks after transplantation. Nuclei were counterstained with DAPI (blue). (F) Levels of human ALB in recipient mouse serum were measured 2 weeks after transplantation. **P*<0.05, ***P*<0.01 (compared with Ad-LacZ-transduced or si-control-transfected cells). Error bars indicate s.d. Statistical analysis was performed using the unpaired two-tailed Student's *t*-test (n=3).

ChIP experiments showed that c/EBPα or c/EBPβ is recruited to the *TGFBR2* promoter region containing the c/EBP binding site in hepatocyte-like cells or cholangiocyte-like cells, respectively (Fig. 5A), suggesting that c/EBPα and c/EBPβ oppositely regulate *TGFBR2* promoter activity in the differentiation from HBCs. We confirmed that c/EBPα or c/EBPβ was mainly recruited to the *TGFBR2* promoter region containing the c/EBP binding site in TGFBR-negative or TGFBR2-positive cells, respectively (supplementary material Fig. S7D). Taken together, we concluded that c/EBPα and c/EBPβ are able to regulate the cell fate decision of HBCs via regulation of TGFBR2 expression. During differentiation from HBCs, *TGFBR2* expression was negatively regulated by c/EBPα and positively regulated by c/EBPβ (Fig. 5B). To examine whether c/EBPα or c/EBPβ could regulate the differentiation from HBCs, *in vitro* gain- and loss-of-function analyses were performed. si-c/EBPα transfection downregulated hepatocyte marker gene expression, whereas it upregulated cholangiocyte marker genes (Fig. 5C). By contrast, si-c/EBPβ transfection upregulated hepatocyte marker and downregulated cholangiocyte marker gene expression (Fig. 5C). In accordance, Ad-c/EBPα transduction upregulated hepatocyte marker genes and downregulated cholangiocyte markers (Fig. 5D), whereas Ad-c/EBPβ transduction downregulated hepatocyte markers and upregulated cholangiocyte marker genes. Promotion of hepatocyte differentiation by Ad-c/EBPα transduction was inhibited by Ad-TGFBR2 transduction, whereas inhibition of cholangiocyte differentiation by Ad-c/EBPα transduction was rescued by Ad-TGFBR2 transduction (Fig. 5E). In addition, promotion of hepatocyte differentiation by si-c/EBPβ transfection was inhibited by Ad-TGFBR2 transduction, whereas inhibition of cholangiocyte differentiation by si-c/EBPβ transfection was rescued by Ad-TGFBR2 transduction (Fig. 5F). We further confirmed that inhibition of hepatocyte differentiation by si-c/EBPα-transfection was rescued by si-TGFBR2 transfection (supplementary material Fig. S8). Taken together, these results led us to conclude that c/EBPα and c/EBPβ could determine the cell fate of HBCs by negatively and positively regulating TGFBR2 expression, respectively (supplementary material Fig. S9).

c/EBPs organize the differentiation of fetal mouse hepatoblasts through regulation of TGFBR2 expression

We have demonstrated that c/EBPs may determine the HBC fate decision via regulation of the expression level of TGFBR2. To examine whether our findings could be replicated in native liver

Development (2014) doi:10.1242/dev.103168

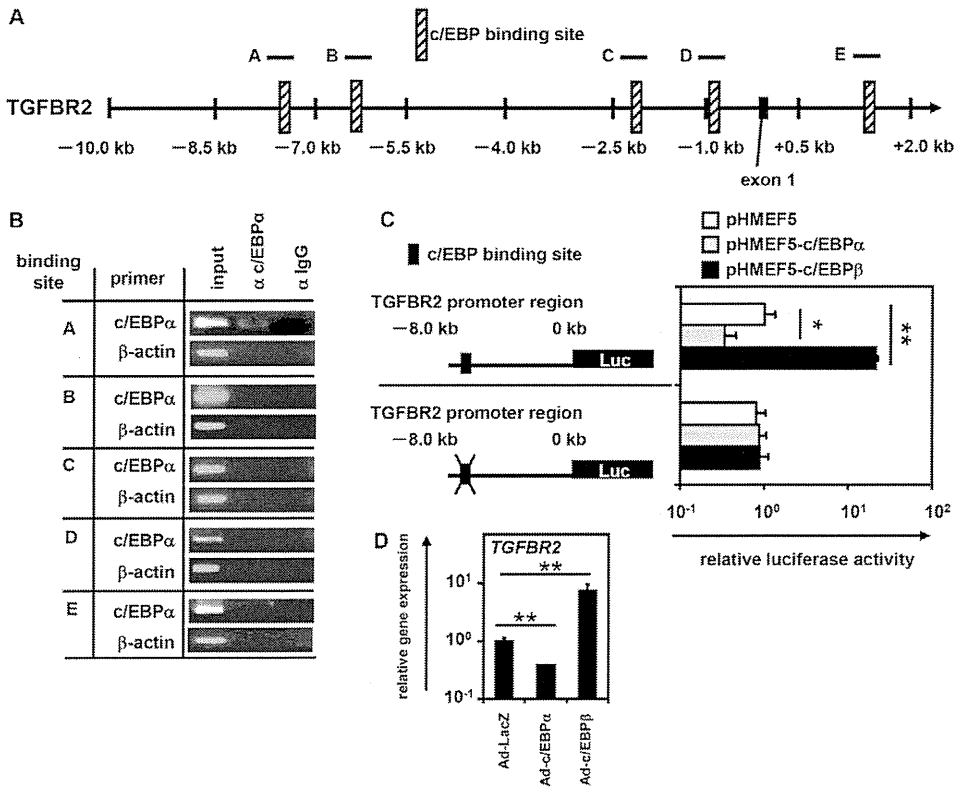

Fig. 4. *TGFBR2* promoter activity and expression are negatively regulated by c/EBPα and positively regulated by c/EBPβ. (A) Candidate c/EBP binding sites (hatched boxes) in the *TGFBR2* promoter region as predicted using rVista 2.0 (see supplementary material Fig. S7). (B) hESCs (H9 cells) were differentiated into hepatoblasts and then a ChIP assay performed. The antibodies and primers employed are summarized in supplementary material Tables S1 and S4. (C) HEK293 cells were transfected with firefly luciferase (Luc) expression plasmids containing the promoter region of *TGFBR2*. In addition, empty plasmid (pHMEF5), c/EBPα expression plasmid (pHMEF5-c/EBPα) or c/EBPβ expression plasmid (pHMEF5-c/EBPβ) was transfected. After 36 hours, a dual luciferase assay was performed. Base pair positions are relative to the translation start site (+1). (D) HepG2 cells (TGFBR2-positive cells) were transduced with 3000 VPs/cell of Ad-LacZ, Ad-c/EBPα or Ad-c/EBPβ for 1.5 hours and cultured for 48 hours. The expression level of *TGFBR2* in HepG2 cells was measured by real-time RT-PCR. On the *y*-axis, the gene expression level in Ad-LacZ-transduced cells was taken as 1.0. $^{*}P<0.05$, $^{**}P<0.01$. Error bars indicate s.d. Statistical analysis was performed using the unpaired two-tailed Student's *t*-test ($n=3$).

development, fetal hepatoblasts were purified from E13.5 mice. The gene expression level of *TGFBR2* in fetal mouse hepatoblasts was negatively or positively regulated by c/EBPα or c/EBPβ, respectively (Fig. 6A,B). The promotion of hepatocyte differentiation by Ad-c/EBPα transduction was inhibited by Ad-TGFBR2 transduction, whereas the inhibition of cholangiocyte differentiation by Ad-c/EBPα transduction was rescued by Ad-TGFBR2 transduction (Fig. 6C). In addition, the promotion of hepatocyte differentiation by si-c/EBPβ transfection was inhibited by Ad-TGFBR2 transduction, whereas the inhibition of cholangiocyte differentiation by si-c/EBPβ transfection was rescued by Ad-TGFBR2 transduction (Fig. 6D). Taken together, these results led us to conclude that c/EBPα and c/EBPβ could determine the cell fate of fetal mouse hepatoblasts by negatively and positively regulating TGFBR2 expression, respectively. Our *in vitro* differentiation system could also prove useful in elucidating the molecular mechanisms of human liver development.

DISCUSSION

The purpose of this study was to better understand the molecular mechanisms of the hepatoblast fate decision in humans. To elucidate the molecular mechanisms of liver development, both conditional knockout mouse models and cell culture systems are useful. For example, DeLaForest et al. demonstrated the role of HNF4α in hepatocyte differentiation using hESC culture systems (DeLaForest et al., 2011). The technology for inducing hepatocyte differentiation from hESCs has recently been dramatically advanced (Takayama et al., 2012a). Because it is possible to generate functional HBCs from hESCs, which can self-replicate and differentiate into both hepatocyte and cholangiocyte lineages (supplementary material Fig. S1 and Fig. 1), the differentiation model of HBCs generated from hESCs should provide a powerful tool for analyzing the molecular mechanisms of human liver development.

In this study, the molecular mechanisms of the hepatoblast fate decision were elucidated using hESC culture systems. HBCs cultured on human LN111 expressed hepatoblast markers (supplementary material Fig. S1) and had the ability to differentiate into both hepatocyte-like cells and cholangiocyte-like cells (Fig. 1). Because a previous study showed that low and high concentrations of TGFβ were required for hepatocyte and cholangiocyte differentiation, respectively (Clotman et al., 2005), we expected that TGFBR2 might contribute to the hepatoblast fate decision. Although TGFβ1, β2 and β3 are all ligands of TGFBR2, TGFβ3 did not promote cholangiocyte differentiation (Fig. 2). This might have been because only TGFβ3 is unable to upregulate the expression of *SOX9*, which is the key factor in bile duct development *in vivo* and cholangiocyte differentiation *in vitro* (Antoniou et al., 2009). We examined the function of TGFBR2 in the hepatoblast fate decision, and found that its overexpression promoted cholangiocyte differentiation, whereas TGFBR2 knockdown promoted hepatocyte differentiation (Fig. 3). Although an exogenous TGFβ ligand was not added to the differentiation medium, the endogenous TGFβ ligand present in Matrigel, which was used in our differentiation protocol, might have bound to TGFBR2. It might also be that the cells committed to the biliary lineage express TGFβ, as a previous study showed that bile duct epithelial cells express TGFβ (Lewindon et al., 2002).

To examine the molecular mechanism regulating TGFBR2 expression, the *TGFBR2* promoter region was analyzed (Fig. 4). *TGFBR2* promoter activity was negatively regulated by c/EBPα and positively regulated by c/EBPβ. c/EBPα overexpression downregulated *TGFBR2* promoter activity in spite of the fact that c/EBPα protein has no repression domain (Yoshida et al., 2006). CTBP1 and CTBP2 (Vernochet et al., 2009) are known to be co-repressors of c/EBPα, and as such constitute candidate co-repressors recruited to the c/EBP binding site in the *TGFBR2* promoter region.

Development (2014) doi:10.1242/dev.103168

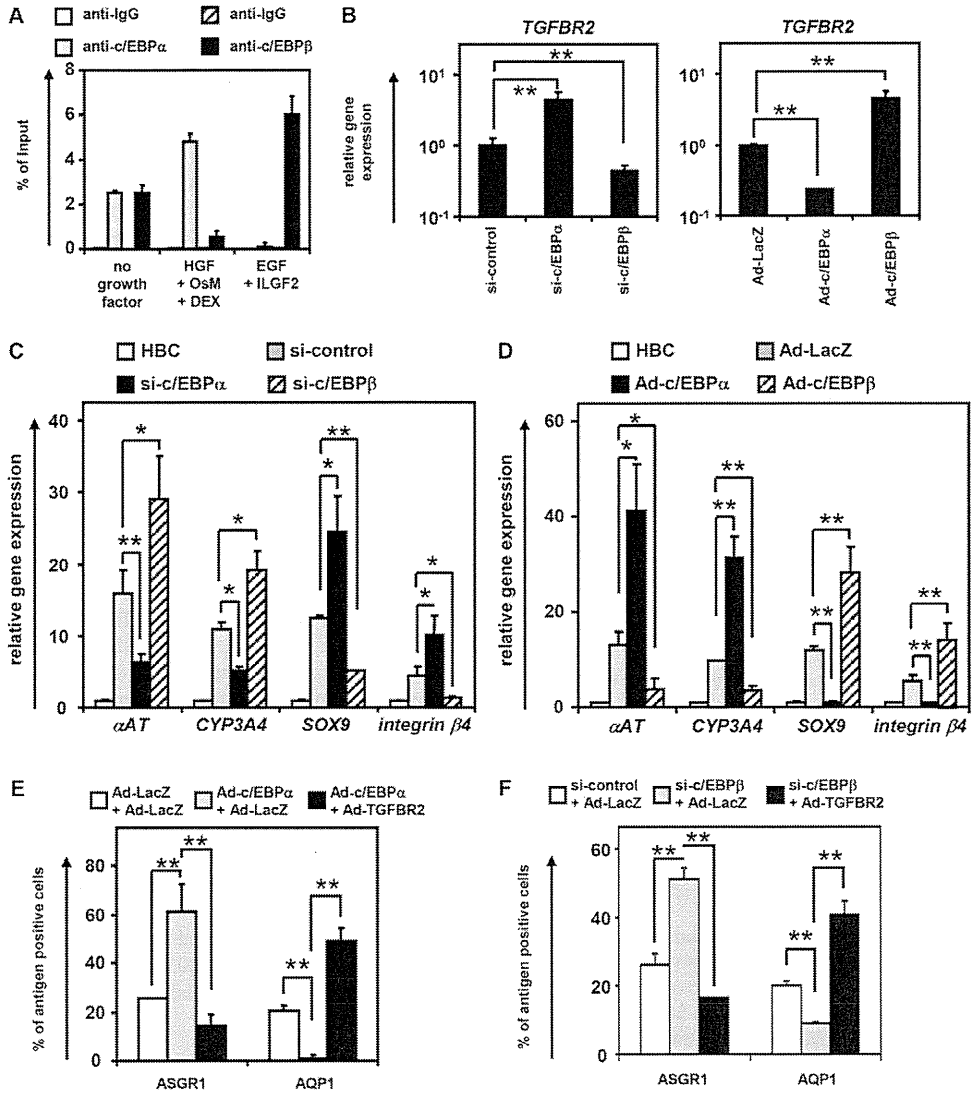

Fig. 5. c/EBPα and c/EBPβ promote hepatocyte and cholangiocyte differentiation by regulating *TGFBR2* expression, respectively. (A) HBCs were differentiated into hepatocyte-like cells or cholangiocyte-like cells according to the scheme outlined in Fig. 1A. On day 10 after hepatocyte or cholangiocyte differentiation, recruitment of c/EBPα or c/EBPβ to the *TGFBR2* promoter region was examined by ChIP assay. (B-D) HBCs were transfected with 50 nM si-control, si-c/EBPα or si-c/EBPβ and cultured in differentiation hESF-DIF medium for 10 days (B left, C). The expression levels of *TGFBR2* and hepatocyte and cholangiocyte markers were then measured by real-time RT-PCR. (B right, D) HBCs were transduced with 3000 VPs/cell of Ad-LacZ, Ad-c/EBPα or Ad-c/EBPβ for 1.5 hours and cultured in differentiation hESF-DIF medium for 10 days. The expression levels of *TGFBR2* and hepatocyte and cholangiocyte markers were then measured by real-time RT-PCR. On the *y*-axis, the gene expression level in the si-control-transfected or Ad-LacZ-transduced cells was taken as 1.0 in B, and levels in HBCs were taken as 1.0 in C and D. (E) HBCs were transduced with 3000 VPs/cell each of Ad-LacZ + Ad-LacZ, Ad-c/EBPα + Ad-LacZ, or Ad-c/EBPα + Ad-TGFBR2 for 1.5 hours and cultured in differentiation hESF-DIF medium for 10 days. The efficiency of hepatocyte or cholangiocyte differentiation was measured by estimating the percentage of ASGR1-positive or AQP1-positive cells, respectively, by FACS analysis. (F) HBCs were transduced with 3000 VPs/cell of Ad-LacZ or Ad-TGFBR2 and then transfected with 50 nM si-control or si-c/EBPβ and cultured in hESF-DIF medium for 10 days. The efficiency of hepatocyte or cholangiocyte differentiation was measured by estimating the percentage of ASGR1-positive or AQP1-positive cells, respectively, by FACS analysis. **P*<0.05, ***P*<0.01. Error bars indicate s.d. Statistical analysis was performed using the unpaired two-tailed Student's *t*-test (*n*=3).

Proteome analysis of c/EBPα would provide an opportunity to identify the co-repressor of c/EBPα. Because large numbers of nearly homogeneous hepatoblasts can be differentiated from hESCs, as compared with the isolation of fetal liver hepatoblasts, hepatocyte differentiation technology from hESCs might prove useful in proteome analysis.

We found that Ad-c/EBPα transduction could promote hepatocyte differentiation by suppressing TGFBR2 expression (Fig. 5). Our findings might thus provide a detailed explanation of the phenotype of *c/EBPα* knockout mice; that is, hepatocyte differentiation is inhibited and cholangiocyte differentiation is promoted in these mice (Yamasaki et al., 2006). We also found that Ad-c/EBPβ transduction could promote cholangiocyte differentiation by enhancing TGFBR2 expression. Because both c/EBPα and c/EBPβ can bind to the same binding site, reciprocal competition for binding is likely to be influenced by regulating c/EBPα or c/EBPβ expression. Therefore, the expression ratio between c/EBPα and c/EBPβ might determine the cell fate of hepatoblasts by regulating the expression level of TGFBR2. We confirmed that our findings could be reproduced in fetal mouse hepatoblasts (Fig. 6). Because a previous study had

Development (2014) doi:10.1242/dev.103168

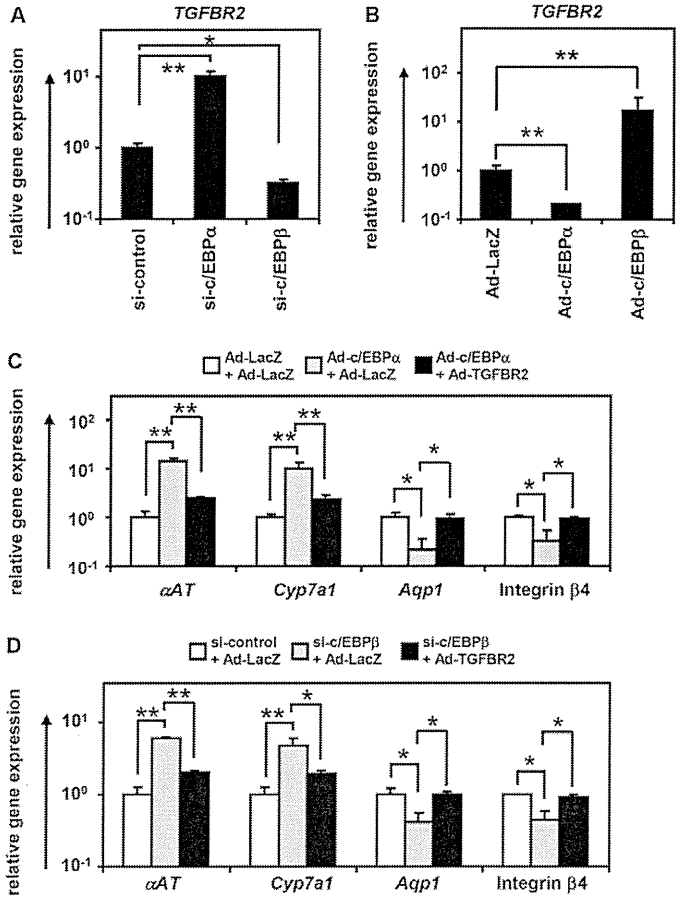

Fig. 6. c/EBPs control the differentiation of fetal mouse hepatoblasts through regulation of TGFBR2 expression. Fetal mouse hepatoblasts (Dlk1-positive cells; the purity was over 98%) were sorted from E13.5 mouse liver. (A) Fetal mouse hepatoblasts were transfected with 50 nM si-control, si-c/EBPα or si-c/EBPβ and cultured for 5 days. The expression of *TGFBR2* was measured by real-time RT-PCR. (B) Fetal mouse hepatoblasts were transduced with 3000 VPs/cell of Ad-LacZ, Ad-c/EBPα or Ad-c/EBPβ for 1.5 hours and cultured for 5 days. The expression of *TGFBR2* was measured by real-time RT-PCR. On the *y*-axis, the gene expression level in the si-control-transfected cells or Ad-LacZ-transduced cells was taken as 1.0. (C) Fetal mouse hepatoblasts were transduced with 3000 VPs/cell each of Ad-LacZ + Ad-LacZ, Ad-c/EBPα + Ad-LacZ, or Ad-c/EBPα + Ad-TGFBR2 for 1.5 hours and cultured for 5 days. On day 5, the expression levels of hepatocyte (*αAT* and *Cyp7a1*) and cholangiocyte (*Aqp1* and integrin β4) markers were measured by real-time RT-PCR. (D) Fetal mouse hepatoblasts were transduced with 3000 VPs/cell of Ad-LacZ or Ad-TGFBR2 and then transfected with 50 nM si-control or si-c/EBPβ and cultured for 5 days. On day 5, the gene levels of hepatocyte (*αAT* and *Cyp7a1*) and cholangiocyte (*Aqp1* and integrin β4) markers were measured by real-time RT-PCR. On the *y*-axis, the gene expression level in the si-control-transfected or Ad-LacZ-transduced cells was taken as 1.0. **P*<0.05, ***P*<0.01. Error bars indicate s.d. Statistical analysis was performed using the unpaired two-tailed Student's *t*-test (*n*=3).

shown that the addition of hepatocyte growth factor (HGF) to hepatoblasts upregulated the expression of c/EBPα and downregulated the expression of c/EBPβ (Suzuki et al., 2003), the ratio between c/EBPα and c/EBPβ might be determined by HGF during hepatocyte differentiation.

In this study, we have identified for the first time that *TGFBR2* is a target of c/EBPs in the hepatoblast fate decision (supplementary material Fig. S9). c/EBPα promotes hepatocyte differentiation by downregulating the expression of TGFBR2, whereas c/EBPβ promotes cholangiocyte differentiation by upregulating TGFBR2 expression. This study might have revealed a molecular mechanism underlying the lineage commitment of human hepatoblasts controlled by a gradient of TGFβ signaling. We believe that similar procedures that adopt the model of human pluripotent stem cell (including human iPS cell) differentiation will be used not only for the elucidation of molecular mechanisms underlying human hepatocyte and biliary differentiation but also for investigating the causes of congenital anomalies of the human liver and biliary tract.

MATERIALS AND METHODS

Ad vectors

Ad vectors were constructed by an improved *in vitro* ligation method (Mizuguchi and Kay, 1998; Mizuguchi and Kay, 1999). The human *c/EBPα* and *c/EBPβ* genes (accession numbers NM_004364 and NM_005194, respectively) were amplified by PCR using the following primers: c/EBPα, Fwd 5′-GCTCTAGATGCCGGGAGAACTCTAACTC-3′ and Rev 5′-GCGGTACCAAACCACTCCCTGGGTCC-3′; c/EBPβ, Fwd 5′-GCATCTAGATTCATGCAACGCCTGGTG-3′ and Rev 5′-ATAGGTACCTAAAATTACCGACGGGCTCC-3′. The human *TGFBR2* gene was purchased from Addgene (plasmid 16622). The human *c/EBPα*, *c/EBPβ* or *TGFBR2* gene was inserted into pBSKII (Invitrogen), resulting in pBSKII-c/EBPα, -c/EBPβ or -TGFBR2. Then, human *c/EBPα*, *c/EBPβ* or *TGFBR2* was inserted into pHMEF5 (Kawabata et al., 2005), which contains the human elongation factor 1α (*EF1α*, also known as *EEF1A1*) promoter, resulting in pHMEF5-c/EBPα, -c/EBPβ or -TGFBR2. pHMEF5-c/EBPα, -c/EBPβ or -TGFBR2 was digested with I-*Ceu*I/PI-*Sce*I and ligated into I-*Ceu*I/PI-*Sce*I-digested pAdHM41-K7 (Koizumi et al., 2003), resulting in pAd-c/EBPα, -c/EBPβ or -TGFBR2. The human *EF1α* promoter-driven *lacZ*- or FOXA2-expressing Ad vectors (Ad-LacZ or Ad-FOXA2, respectively) were constructed previously (Takayama et al., 2012b; Tashiro et al., 2008). All Ad vectors contain a stretch of lysine residues (K7) in the C-terminal region of the fiber knob for more efficient transduction of hESCs, definitive endoderm cells and HBCs, in which transfection efficiency was almost 100%, and the Ad vectors were purified as described previously (Takayama et al., 2012a; Takayama et al., 2011). The vector particle (VP) titer was determined by a spectrophotometric method (Maizel et al., 1968).

hESC culture

The H9 hESC line (WiCell Research Institute) was maintained on a feeder layer of mitomycin C-treated mouse embryonic fibroblasts (Merck Millipore) in ReproStem medium (ReproCELL) supplemented with 5 ng/ml FGF2 (Katayama Kagaku Kogyo). H9 was used following the Guidelines for Derivation and Utilization of Human Embryonic Stem Cells of the Ministry of Education, Culture, Sports, Science and Technology of Japan and the study was approved by the Independent Ethics Committee.

Generation and maintenance of hESC-derived HBCs

Before the initiation of cellular differentiation, the hESC medium was exchanged for a defined serum-free medium, hESF9, and cultured as previously reported (Furue et al., 2008). The differentiation protocol for the induction of definitive endoderm cells and HBCs was based on our previous reports with some modifications (Takayama et al., 2012a; Takayama et al., 2012b; Takayama et al., 2011). Briefly, in mesendoderm differentiation, hESCs were cultured for 2 days on Matrigel Matrix (BD Biosciences) in differentiation hESF-DIF medium, which contains 100 ng/ml activin A (R&D Systems); hESF-DIF medium was purchased from Cell Science & Technology Institute; differentiation hESF-DIF medium was supplemented with 10 μg/ml human recombinant insulin, 5 μg/ml human apotransferrin, 10 μM 2-mercaptoethanol, 10 μM ethanolamine, 10 μM sodium selenite, 0.5 mg/ml bovine fatty acid-free serum albumin (all from Sigma) and 1×B27 Supplement (without vitamin A; Invitrogen). To generate definitive endoderm cells, the mesendoderm cells were transduced with 3000 VPs/cell of FOXA2-expressing Ad vector (Ad-FOXA2) for 1.5 hours on day 2 and cultured until day 6 on Matrigel in differentiation hESF-DIF medium supplemented with 100 ng/ml activin A. For induction of the HBCs, the

definitive endoderm cells were cultured for 3 days on Matrigel in differentiation hESF-DIF medium supplemented with 20 ng/ml BMP4 (R&D Systems) and 20 ng/ml FGF4 (R&D Systems). Transient overexpression of FOXA2 in the mesendoderm cells is not necessary for establishing HBCs, but it is helpful for efficient generation of the HBCs. The HBCs were first purified from the hESC-derived cells (day 9) by selecting attached cells on a human recombinant LN111 (BioLamina)-coated dish 15 minutes after plating (Takayama et al., 2013). The HBCs were cultured on a human LN111-coated dish (2.0×10^4 cells/cm^2) in maintenance DMEM/F12 medium [DMEM/F12 medium (Invitrogen) supplemented with 10% fetal bovine serum (FBS), 1× insulin/transferrin/selenium, 10 mM nicotinamide, 0.1 μM dexamethasone (DEX) (Sigma), 20 mM HEPES, 25 mM $NaHCO_3$, 2 mM L-glutamine, and penicillin/streptomycin] which contained 40 ng/ml HGF (R&D Systems) and 20 ng/ml epidermal growth factors (EGF) (R&D Systems). The medium was refreshed every day. The HBCs were dissociated with Accutase (Millipore) into single cells, and subcultured every 6 or 7 days. The HBCs used in this study were passaged more than three times.

In vitro hepatocyte and cholangiocyte differentiation

To induce hepatocyte differentiation, the HBCs were cultured on a Matrigel-coated dish (7.5×10^4 cells/cm^2) in Hepatocyte Culture Medium (HCM without EGF; Lonza) supplemented with 20 ng/ml HGF, 20 ng/ml Oncostatin M (OsM) (R&D Systems) and 1 μM DEX. To induce cholangiocyte differentiation, the HBCs were cultured in collagen gel. To establish collagen gel plates, 500 μl collagen gel solution [400 μl type I-A collagen (Nitta gelatin), 50 μl 10× DMEM and 50 μl 200 mM HEPES buffer containing 2.2% $NaHCO_3$ and 0.05 M NaOH] was added to each well, and then the plates were incubated at 37°C for 30 minutes. The HBCs (5×10^4 cells) were resuspended in 500 μl differentiation DMEM/F12 medium [DMEM/F12 medium supplemented with 20 mM HEPES, 2 mM L-glutamine, 100 ng/ml EGF and 40 ng/ml ILGF2 (IGF2)], and then mixed with 500 μl of the collagen gel solution and plated onto the basal layer of collagen. After 30 minutes, 2 ml differentiation DMEM/F12 medium was added to the well.

Inhibition of TGFβ signaling

SB-431542 (Santa Cruz Biotechnology), which is a small molecule that acts as a selective inhibitor of activin receptor-like kinase (ALK) receptors [ALK4, ALK5 and ALK7 (also known as ACVR1B, TGFBR1 and ACVR1C)], was used to inhibit TGFβ signaling in HBCs.

Flow cytometry

Single-cell suspensions of hESC-derived cells were fixed with 2% paraformaldehyde (PFA) at 4°C for 20 minutes, and then incubated with primary antibody (supplementary material Table S1) followed by secondary antibody (supplementary material Table S2). Flow cytometry analysis was performed using a FACS LSR Fortessa flow cytometer (BD Biosciences). Cell sorting was performed using a FACS Aria (BD Biosciences).

RNA isolation and reverse transcription (RT)-PCR

Total RNA was isolated from hESCs and their derivatives using ISOGENE (Nippon Gene). cDNA was synthesized using 500 ng total RNA with the SuperScript VILO cDNA Synthesis Kit (Invitrogen). Real-time RT-PCR was performed with SYBR Green PCR Master Mix (Applied Biosystems) using an Applied Biosystems StemOnePlus real-time PCR system. Relative quantification was performed against a standard curve and the values were normalized against the input determined for the housekeeping gene *GAPDH*. Primers are described in supplementary material Table S3.

Immunohistochemistry

Cells were fixed with 4% PFA. After incubation with 0.1% Triton X-100 (Wako), blocking with Blocking One (Nakalai Tesque) or PBS containing 2% FBS, 2% BSA and 0.1% Triton X-100, the cells were incubated with primary antibody (supplementary material Table S1) at 4°C overnight, followed by secondary antibody (supplementary material Table S2) at room temperature for 1 hour. Immunopositive cells were counted in at least eight randomly chosen fields.

HBC colony formation assay

For the colony formation assay, HBCs were cultured at a low density (200 cells/cm^2) on a human LN111-coated dish in maintenance DMEM/F12 medium supplemented with 25 μM LY-27632 (ROCK inhibitor; Millipore).

Transplantation of clonally derived HBCs

Clonally derived HBCs were dissociated using Accutase and then suspended in maintenance DMEM/F12 medium without serum. The HBCs (1×10^6 cells) were transplanted 24 hours after administration of CCl_4 (2 mg/kg) by intrasplenic injection into 8- to 10-week-old *Rag2/Il2rg* double-knockout mice. Recipient mouse livers and blood were harvested 2 weeks after transplantation. Grafts were fixed with 4% PFA and processed for immunohistochemistry. Serum was extracted and subjected to ELISA. All animal experiments were conducted in accordance with institutional guidelines.

ELISA

Levels of human ALB in mouse serum were examined by ELISA using kits from Bethyl Laboratories according to the manufacturer's instructions.

Culture of mouse Dlk1$^+$ cells

Dlk1$^+$ hepatoblasts were isolated from E13.5 mouse livers using anti-mouse Dlk1 monoclonal antibody (MBL International Corporation, D187-4) as described previously (Tanimizu et al., 2003). Dlk1$^+$ cells were resuspended in DMEM/F12 (Sigma) containing 10% FBS, 1× insulin/transferrin/selenium (ITS), 10 mM nicotinamide (Wako), 0.1 μM DEX and 5 mM L-glutamine. Cells were plated on laminin-coated dishes and cultured in medium containing 20 ng/ml HGF, EGF and 25 μM LY-27632 (ROCK inhibitor).

lacZ assay

Hepatoblasts were transduced with Ad-LacZ at 3000 VPs/cell for 1.5 hours. The day after transduction (day 10), 5-bromo-4-chloro-3-indolyl β-D-galactopyranoside (X-Gal) staining was performed as described previously (Kawabata et al., 2005).

Reporter assays

The effects of c/EBPα or c/EBPβ overexpression on *TGFBR2* promoter activity were examined using a reporter assay. An 8 kb fragment of the 5′ flanking region of the *TGFBR2* gene was amplified by PCR using the following primers: Fwd, 5′-CCGAGCTCATGTTTGATGAAGTGTCTAG-CTTCCAAGG-3′; Rev, 5′-GGCTCGAGCCTCGACGTCCAGCCCCT-3′. The fragment was inserted into the *SacI*/*XhoI* sites of pGL3-basic (Promega), resulting in a pGL3-*TGFBR2* promoter region (pGL3-TGFBR2-PR). To generate a *TGFBR2* promoter region containing mutations in the c/EBP binding site, the following primers were used in PCR (mutations are indicated by lowercase letters): Fwd, 5′-CACTAGTATTCAgTG-AtCcgAAAATATGG-3′; Rev, 5′-CACTAGTATTCAgTGAtCcgAAAA-TATGG-3′; this resulted in pGL3-mTGFBR2-PR. HEK293 cells were maintained in DMEM (Wako) supplemented with 10% FBS, penicillin and streptomycin, and 2 mM L-glutamine. In reporter assays, 60 ng pGL3-TGFBR2-PR or pGL3-mTGFBR2-PR was transfected together with 720 ng each expression plasmid (pHMEF5, pHMEF5-c/EBPα and pHMEF5-c/EBPβ) and 60 ng internal control plasmid (pCMV-Renilla luciferase) using Lipofectamine 2000 reagent (Invitrogen). Transfected cells were cultured for 36 hours, and a Dual Luciferase Assay (Promega) was performed according to the manufacturer's instructions.

siRNA-mediated knockdown

Predesigned siRNAs targeting *c/EBPα*, *c/EBPβ* and *TGFBR2* mRNAs were purchased from Thermo Scientific Dharmacon. Cells were transfected with 50 nM siRNA using RNAiMAX (Invitrogen) transfection reagent according to the manufacturer's instructions. As a negative control, we used scrambled siRNA (Qiagen) of a sequence showing no significant similarity to any mammalian gene.

Chromatin immunoprecipitation (ChIP) assay

The ChIP assay kit was purchased from Upstate. Cells were crosslinked using formaldehyde at a final concentration of 1% at 37°C for 10 minutes, and then genomic DNA was fragmented by sonicator. The resulting DNA-protein complexes were immunoprecipitated using the antibodies described in supplementary material Table S1 or control IgG as described in supplementary material Table S2. The precipitated DNA fragments were analyzed by real-time RT-PCR using the primers shown in supplementary material Table S4 to amplify the *TGFBR2* promoter region including the c/EBP binding sites or β-actin locus as a control. The results of quantitative ChIP analysis (Fig. 5A) were expressed as the amount of amplified *TGFBR2* promoter region relative to input DNA taken as 100%.

Statistical analysis

Statistical analysis was performed using an unpaired two-tailed Student's *t*-test. All data are represented as mean ± s.d. (n=3).

Acknowledgements

We thank Natsumi Mimura, Yasuko Hagihara and Hiroko Matsumura for excellent technical support.

Competing interests

The authors declare no competing financial interests.

Author contributions

K. Takayama, K.K. and H.M. developed the concepts or approach; K. Takayama, Y.N., K.O., H.O. and T.Y. performed experiments; K. Takayama, K.K., M.I., K. Tashiro, F.S., T.H., T.O., M.F.K. and H.M. performed data analysis; K. Takayama, K.K. and H.M. prepared or edited the manuscript prior to submission.

Funding

H.M., K.K., M.K.F. and T.H. were supported by grants from the Ministry of Health, Labor, and Welfare of Japan (MEXT). H.M. was also supported by Japan Research Foundation for Clinical Pharmacology, The Uehara Memorial Foundation. K.O. was supported by Special Coordination Funds for Promoting Science and Technology from MEXT. F.S. was supported by Program for Promotion of Fundamental Studies in Health Sciences of the National Institute of Biomedical Innovation (NIBIO). K. Takayama and Y.N. are Research Fellows of the Japan Society for the Promotion of Science.

Supplementary material

Supplementary material available online at
http://dev.biologists.org/lookup/suppl/doi:10.1242/dev.103168/-/DC1

References

Agarwal, S., Holton, K. L. and Lanza, R. (2008). Efficient differentiation of functional hepatocytes from human embryonic stem cells. *Stem Cells* **26**, 1117-1127.

Antoniou, A., Raynaud, P., Cordi, S., Zong, Y., Tronche, F., Stanger, B. Z., Jacquemin, P., Pierreux, C. E., Clotman, F. and Lemaigre, F. P. (2009). Intrahepatic bile ducts develop according to a new mode of tubulogenesis regulated by the transcription factor SOX9. *Gastroenterology* **136**, 2325-2333.

Chen, S. S., Chen, J. F., Johnson, P. F., Muppala, V. and Lee, Y. H. (2000). C/EBPbeta, when expressed from the C/ebpalpha gene locus, can functionally replace C/EBPalpha in liver but not in adipose tissue. *Mol. Cell. Biol.* **20**, 7292-7299.

Clotman, F., Jacquemin, P., Plumb-Rudewiez, N., Pierreux, C. E., Van der Smissen, P., Dietz, H. C., Courtoy, P. J., Rousseau, G. G. and Lemaigre, F. P. (2005). Control of liver cell fate decision by a gradient of TGF beta signaling modulated by Onecut transcription factors. *Genes Dev.* **19**, 1849-1854.

DeLaForest, A., Nagaoka, M., Si-Tayeb, K., Noto, F. K., Konopka, G., Battle, M. A. and Duncan, S. A. (2011). HNF4A is essential for specification of hepatic progenitors from human pluripotent stem cells. *Development* **138**, 4143-4153.

Furue, M. K., Na, J., Jackson, J. P., Okamoto, T., Jones, M., Baker, D., Hata, R., Moore, H. D., Sato, J. D. and Andrews, P. W. (2008). Heparin promotes the growth of human embryonic stem cells in a defined serum-free medium. *Proc. Natl. Acad. Sci. USA* **105**, 13409-13414.

Hansen, A. J., Lee, Y. H., Sterneck, E., Gonzalez, F. J. and Mackenzie, P. I. (1998). C/EBPalpha is a regulator of the UDP glucuronosyltransferase UGT2B1 gene. *Mol. Pharmacol.* **53**, 1027-1033.

Kawabata, K., Sakurai, F., Yamaguchi, T., Hayakawa, T. and Mizuguchi, H. (2005). Efficient gene transfer into mouse embryonic stem cells with adenovirus vectors. *Mol. Ther.* **12**, 547-554.

Kitisin, K., Saha, T., Blake, T., Golestaneh, N., Deng, M., Kim, C., Tang, Y., Shetty, K., Mishra, B. and Mishra, L. (2007). Tgf-Beta signaling in development. *Sci. STKE* **2007**, cm1.

Koizumi, N., Mizuguchi, H., Utoguchi, N., Watanabe, Y. and Hayakawa, T. (2003). Generation of fiber-modified adenovirus vectors containing heterologous peptides in both the HI loop and C terminus of the fiber knob. *J. Gene Med.* **5**, 267-276.

Lewindon, P. J., Pereira, T. N., Hoskins, A. C., Bridle, K. R., Williamson, R. M., Shepherd, R. W. and Ramm, G. A. (2002). The role of hepatic stellate cells and transforming growth factor-beta(1) in cystic fibrosis liver disease. *Am. J. Pathol.* **160**, 1705-1715.

Maizel, J. V., Jr, White, D. O. and Scharff, M. D. (1968). The polypeptides of adenovirus. I. Evidence for multiple protein components in the virion and a comparison of types 2, 7A, and 12. *Virology* **36**, 115-125.

Mizuguchi, H. and Kay, M. A. (1998). Efficient construction of a recombinant adenovirus vector by an improved in vitro ligation method. *Hum. Gene Ther.* **9**, 2577-2583.

Mizuguchi, H. and Kay, M. A. (1999). A simple method for constructing E1- and E1/E4-deleted recombinant adenoviral vectors. *Hum. Gene Ther.* **10**, 2013-2017.

Oe, S., Lemmer, E. R., Conner, E. A., Factor, V. M., Levéen, P., Larsson, J., Karlsson, S. and Thorgeirsson, S. S. (2004). Intact signaling by transforming growth factor beta is not required for termination of liver regeneration in mice. *Hepatology* **40**, 1098-1105.

Plumb-Rudewiez, N., Clotman, F., Strick-Marchand, H., Pierreux, C. E., Weiss, M. C., Rousseau, G. G. and Lemaigre, F. P. (2004). Transcription factor HNF-6/OC-1 inhibits the stimulation of the HNF-3alpha/Foxa1 gene by TGF-beta in mouse liver. *Hepatology* **40**, 1266-1274.

Schmelzer, E., Zhang, L., Bruce, A., Wauthier, E., Ludlow, J., Yao, H. L., Moss, N., Melhem, A., McClelland, R., Turner, W. et al. (2007). Human hepatic stem cells from fetal and postnatal donors. *J. Exp. Med.* **204**, 1973-1987.

Suzuki, A., Iwama, A., Miyashita, H., Nakauchi, H. and Taniguchi, H. (2003). Role for growth factors and extracellular matrix in controlling differentiation of prospectively isolated hepatic stem cells. *Development* **130**, 2513-2524.

Takayama, K., Inamura, M., Kawabata, K., Tashiro, K., Katayama, K., Sakurai, F., Hayakawa, T., Furue, M. K. and Mizuguchi, H. (2011). Efficient and directive generation of two distinct endoderm lineages from human ESCs and iPSCs by differentiation stage-specific SOX17 transduction. *PLoS ONE* **6**, e21780.

Takayama, K., Inamura, M., Kawabata, K., Katayama, K., Higuchi, M., Tashiro, K., Nonaka, A., Sakurai, F., Hayakawa, T., Furue, M. K. et al. (2012a). Efficient generation of functional hepatocytes from human embryonic stem cells and induced pluripotent stem cells by HNF4α transduction. *Mol. Ther.* **20**, 127-137.

Takayama, K., Inamura, M., Kawabata, K., Sugawara, M., Kikuchi, K., Higuchi, M., Nagamoto, Y., Watanabe, H., Tashiro, K., Sakurai, F. et al. (2012b). Generation of metabolically functioning hepatocytes from human pluripotent stem cells by FOXA2 and HNF1α transduction. *J. Hepatol.* **57**, 628-636.

Takayama, K., Nagamoto, Y., Mimura, N., Tashiro, K., Sakurai, F., Tachibana, M., Hayakawa, T., Kawabata, K. and Mizuguchi, H. (2013). Long-term self-renewal of human ES/iPS-derived hepatoblast-like cells on human laminin 111-coated dishes. *Stem Cell Reports* **1**, 322-335.

Tanimizu, N., Nishikawa, M., Saito, H., Tsujimura, T. and Miyajima, A. (2003). Isolation of hepatoblasts based on the expression of Dlk/Pref-1. *J. Cell Sci.* **116**, 1775-1786.

Tashiro, K., Kawabata, K., Sakurai, H., Kurachi, S., Sakurai, F., Yamanishi, K. and Mizuguchi, H. (2008). Efficient adenovirus vector-mediated PPAR gamma gene transfer into mouse embryoid bodies promotes adipocyte differentiation. *J. Gene Med.* **10**, 498-507.

Tomizawa, M., Garfield, S., Factor, V. and Xanthopoulos, K. G. (1998). Hepatocytes deficient in CCAAT/enhancer binding protein alpha (C/EBP alpha) exhibit both hepatocyte and biliary epithelial cell character. *Biochem. Biophys. Res. Commun.* **249**, 1-5.

Vernochet, C., Peres, S. B., Davis, K. E., McDonald, M. E., Qiang, L., Wang, H., Scherer, P. E. and Farmer, S. R. (2009). C/EBPalpha and the corepressors CtBP1 and CtBP2 regulate repression of select visceral white adipose genes during induction of the brown phenotype in white adipocytes by peroxisome proliferator-activated receptor gamma agonists. *Mol. Cell. Biol.* **29**, 4714-4728.

Yamasaki, H., Sada, A., Iwata, T., Niwa, T., Tomizawa, M., Xanthopoulos, K. G., Koike, T. and Shiojiri, N. (2006). Suppression of C/EBPalpha expression in periportal hepatoblasts may stimulate biliary cell differentiation through increased Hnf6 and Hnf1b expression. *Development* **133**, 4233-4243.

Yoshida, Y., Hughes, D. E., Rausa, F. M., III, Kim, I. M., Tan, Y., Darlington, G. J. and Costa, R. H. (2006). C/EBPalpha and HNF6 protein complex formation stimulates HNF6-dependent transcription by CBP coactivator recruitment in HepG2 cells. *Hepatology* **43**, 276-286.

STEM CELLS®

EMBRYONIC STEM CELLS/INDUCED PLURIPOTENT STEM CELLS

Molecular Functions of the LIM-Homeobox Transcription Factor *Lhx2* in Hematopoietic Progenitor Cells Derived from Mouse Embryonic Stem Cells

KENJI KITAJIMA,[a] MANAMI KAWAGUCHI,[a] MICHELINA IACOVINO,[b] MICHAEL KYBA,[b] TAKAHIKO HARA[a]*

[a]Stem Cell Project Group, Tokyo Metropolitan Institute of Medical Science, Tokyo, Japan; [b]Lillehei Heart Institute, Department of Pediatrics, University of Minnesota, Minneapolis, Minnesota, USA

Key Words. Hematopoietic stem cells • Embryonic stem cells • In vitro differentiation • LIM-homeobox transcription factor • Lhx2 • OP9

ABSTRACT

We previously demonstrated that hematopoietic stem cell (HSC)-like cells are robustly expanded from mouse embryonic stem cells (ESCs) by enforced expression of Lhx2, a LIM-homeobox domain (LIM-HD) transcription factor. In this study, we analyzed the functions of Lhx2 in that process using an ESC line harboring an inducible *Lhx2* gene cassette. When ESCs are cultured on OP9 stromal cells, hematopoietic progenitor cells (HPCs) are differentiated and these HPCs are prone to undergo rapid differentiation into mature hematopoietic cells. Lhx2 inhibited differentiation of HPCs into mature hematopoietic cells and this effect would lead to accumulation of HSC-like cells. LIM-HD factors interact with LIM domain binding (Ldb) protein and this interaction abrogates binding of LIM-only (Lmo) protein to Ldb. We found that one of Lmo protein, Lmo2, was unstable due to dissociation of Lmo2 from Ldb1 in the presence of Lhx2. This effect of Lhx2 on the amount of Lmo2 contributed into accumulation of HSC-like cells, since enforced expression of Lmo2 into HSC-like cells inhibited their self-renewal. Expression of *Gata3* and *Tal1/Scl* was increased in HSC-like cells and enforced expression of Lmo2 reduced expression of *Gata3* but not *Tal1/Scl*. Enforced expression of Gata3 into HPCs inhibited mature hematopoietic cell differentiation, whereas *Gata3*-knockdown abrogated the Lhx2-mediated expansion of HPCs. We propose that multiple transcription factors/cofactors are involved in the Lhx2-mediated expansion of HSC-like cells from ESCs. Lhx2 appears to fine-tune the balance between self-renewal and differentiation of HSC-like cells. STEM CELLS *2013;31:2680–2689*

Disclosure of potential conflicts of interest is found at the end of this article.

INTRODUCTION

Hematopoiesis is a tissue stem cell-based process by which hematopoietic stem cells (HSCs) differentiate into more than 10 types of mature blood cells [1]. HSCs have multilineage differentiation and self-renewal capabilities. During differentiation, HSCs exit G0 phase, proliferate, and differentiate into hematopoietic progenitor cells (HPCs) that have lineage-specific differentiation potentials and give rise to terminally differentiated mature blood cells. The differentiation of HSCs is elegantly controlled by environmental cues and intrinsic genetic programs. The bone marrow niche is important for regulating the self-renewal, survival, and differentiation of HSCs [2]. Conversely, intrinsic genetic programs that maintain the characteristics of HSCs are controlled by several transcription factors and epigenetic modifiers [3, 4]. Transcriptional networks comprising these factors cooperatively and antagonistically control the fate of HSCs.

Homeobox transcription factors play crucial roles in embryogenesis. The homeobox domain (HD) is a highly conserved protein motif that can bind DNA. Among which, members of the LIM-HD transcription factor protein family possess a LIM domain comprised of two zinc finger-like structures in their N-terminal region. The LIM domain recognizes a variety of transcriptional cofactors. LIM domain binding protein (Ldb) 1 and 2 modulate the molecular and biological functions of LIM-HD proteins [5, 6].

Lhx2 (also known as LH2) is a LIM-HD factor that has been originally identified in pituitary cells and in pre-B-cell lines [7, 8]. Lhx2 expression is essential in a wide variety of progenitor/stem cell populations. *Lhx2*-null mice revealed that Lhx2 has indispensable roles in the brain, the eye, and definitive hematopoiesis [9]. Additionally, Lhx2 acts on stem cells

Contract grant sponsor: Grants-in-Aid for Scientific Research from the Ministry of Education, Culture, Sports, Science, and Technology of Japan; Contract grant number: 24591415 to K.K. and 23390256 to K.K. and T.H.
Contract grant sponsor: SENSHIN Medical Research Foundation.

Author contributions: K.K.: conception and design, collection and assembly of data, data analysis and interpretation, and manuscript writing; M.Ka.: collection and assembly of data; M.I., M.Ky.: provision of study material; T.H.: conception and design and manuscript writing.

Correspondence: Kenji Kitajima, Ph.D., Stem Cell Project Group, Tokyo Metropolitan Institute of Medical Science, 2-1-6 Kamikitazawa, Setagaya-ku, Tokyo 156-8506, Japan. Telephone: 81-3-5316-3130; Fax: 81-3-5316-3226; e-mail: kitajima-kj@igakuken.or.jp Correspondence: Takahiko Hara, Ph.D., Stem Cell Project Group, Tokyo Metropolitan Institute of Medical Science, 2-1-6 Kamikitazawa, Setagaya-ku, Tokyo 156–8506, Japan. Telephone: 81-3-5316-3130; Fax: +81-3-5316-3226; e-mail: hara-tk@igakuken.or.jp Received February 26, 2013; accepted for publication July 5, 2013; first published online in STEM CELLS *EXPRESS* August 6, 2013. 1066-5099/2013/$30.00/0 doi: 10.1002/stem.1500

in hair follicles to preserve the postnatal bulge compartment [10]. *Lhx2*-null mouse embryos die in utero with severe anemia, suggesting that Lhx2 has a critical role in hematopoiesis [9]. Lhx2 is aberrantly expressed in several cases of human chronic myelogenous leukemia [11], suggesting that Lhx2 stimulates the growth of immature hematopoietic cells. The effects of Lhx2 on hematopoiesis have been analyzed by enforced expression of Lhx2 in mouse HSCs isolated from adult bone marrow [12], which resulted in the ex vivo expansion of engraftable HSC-like cells. In addition, when *Lhx2* is introduced into mouse embryonic stem cells (ESCs) that are subsequently induced to differentiate via the embryoid body formation method, multipotent HPCs continuously proliferate [13]. These HPCs are mainly composed of c-Kit$^+$/Sca1$^-$/lineage$^-$ (KL) cells, but not c-Kit$^+$/Sca1$^+$/lineage$^-$ (KSL) cells.

We previously explored the consequences of enforced expression of *Lhx2* during hematopoietic differentiation of mouse ESCs in vitro [14]. When the OP9 coculture method is used to induce hematopoietic differentiation of mouse ESCs, expression of Lhx2 results in the expansion of KSL/KL cells. These KSL/KL cells are also amplified from mouse-induced pluripotent stem (iPS) cells. Furthermore, Lhx2-induced KSL/KL cells display long-term hematopoiesis-repopulating (LTR) activity. When transplanted into lethally irradiated congenic mice, Lhx2-induced KSL/KL cells differentiate in vivo over 4 months into multilineage hematopoietic cells such as myeloid cells, erythroid cells, megakaryocytes/platelets, and B cells. Thus, KSL/KL cells induced by retroviral transduction of *Lhx2* displayed HSC-like property. However, T-cell repopulation is hardly detected, suggesting that Lhx2 inhibits T-cell differentiation [14].

Understanding the mechanisms that underlie the expansion of mouse ES-derived KSL/KL cells by Lhx2 would provide invaluable information for the future therapeutic applications of human iPS cells and human cord blood. However, the molecular mechanisms responsible for the dramatic effects of Lhx2 remain unclear. In this study, we demonstrate that overexpression of Lhx2 decreases the amount of Lmo2 (also known as rbtn2) and upregulates *Gata3* expression, both of which are expressed in newly emerged HSCs in the aorta/gonad/mesonephros region of mouse embryos [15]. These changes underlie the accumulation of KSL/KL cells in vitro by overexpression of Lhx2.

Materials and Methods

Cell Culture

Mouse ESCs (RENKA, E14tg2a, Gata1-KO [16], A2Lox-cre [17]) were maintained on mitomycin C-treated mouse embryonic fibroblasts in Dulbecco's modified Eagle's medium (DMEM) (Sigma, St. Louis, MO, www.sigmaaldrich.com) supplemented with 15% knockout serum replacement, 1% fetal bovine serum (FBS, Gibco-Invitrogen, Carlsbad, CA, www.invitrogen.com), penicillin/streptomycin (Pen/Str), nonessential amino acids (Gibco-Invitrogen), sodium pyruvate (Gibco-Invitrogen), 2-mercaptoethanol (Sigma), and 10^3 U/ml ESGro (Gibco-Invitrogen). ESC lines with inducible *Lhx2* (iLhx2-ESCs) and *Gata3* (iGata3-ESCs) expression were generated by transfecting p2Lox-*FLAG-Lhx2* or p2Lox-*Gata3* into A2Lox-cre ESCs, respectively. Cre/loxP-mediated integration of *FLAG-Lhx2* and *Gata3* into the *Hprt* locus was confirmed by genomic PCR. The expression of *Lhx2* and *Gata3* was confirmed by immunofluorescent staining, Western blotting, and reverse transcription (RT)-PCR.

OP9 stromal cells were maintained in alfa-MEM (Gibco-Invitrogen) supplemented with 20% FBS and Pen/Str [18]. Mouse *δ-like 1* (*Dll*) cDNA was cloned from mouse thymus by RT-PCR. OP9-DL1 cells were generated by retroviral transduction of pMY-Dll-IRES-EGFP followed by sorting of EGFP$^+$ cells. Dll expression was confirmed by fluorescence-activated cell sorting (FACS) analysis using an anti-Dll antibody (BioLegend, San Diego, CA, http://www.biolegend.com). 293T cells and Plat-E packaging cells were maintained in DMEM supplemented with 10% FBS and Pen/Str. Retrovirus production was performed by transfecting Plat-E cells with pMY-IRES-EGFP, pMY-Lhx2-IRES-EGFP, pMY-IRES-EYFP, pMY-Lmo2-IRES-EYFP, or pMY-Ldb1-IRES-EYFP using FuGene HD reagent (Promega, Madison, WI, http://www.promega.com). The culture supernatants were collected and used for gene delivery [14]. Lentiviral vectors carrying *EGFP* and short hairpin RNAs (shRNAs) against *Gata3* mRNA were transfected into 293T cells with pMD2G and pCMVR8.91 vectors [19] and supernatants were used for stable introduction of shRNA.

OP9 Coculture of ESCs

Mouse ESC lines (3×10^4 cells) were plated onto confluent OP9 cells in a 60 mm dish on day 0. Half of the culture medium was replaced on day 2 or 3. Cells were detached by treatment with 0.25% trypsin/10 mM EDTA (Sigma) on day 5, and 3×10^5 cells were plated onto fresh confluent OP9 cells or OP9-Dll cells in a 60 mm dish. For expansion of HSC-like cells, interleukin (IL)-6 (10 ng/ml, Peprotech, Rocky Hill, NJ, http://www.peprotech.como) and stem cell factor (SCF) (50 ng/ml, Kirin, Takasaki, Japan, http://www.kirin.co.jp) were added to the culture medium from day 5. Expression of Lhx2 or Gata3 was induced in iLhx2-ESCs or iGata3-ESCs by the addition of 1 μg/ml doxycycline (dox). Hematopoietic cells induced from mouse ESCs were collected by mild pipetting, stained with biotin-lineage cocktail (Miltenyi Biotec, Auburn, CA, http://www.miltenyibiotec.com), phycoerythrin (PE)/Cy7-conjugated anti-c-Kit antibody (BioLegend), and allophycocyanin-conjugated anti-Sca1 antibody (BioLegend), followed by PE-conjugated streptavidin (BioLegend) or PE/Cy5-conjugated streptavidin (BioLegend), and analyzed with a FACSAria cell sorter (BD Pharmingen, Franklin Lakes, NJ, http://www.bd.com). FACS analyses and sorting were carried out as previously described [14]. Retroviral transduction was carried out by spin infection as previously described [14].

Hematopoietic lineage-directed differentiation of ESCs was induced by the addition of cytokines from day 5: 10 ng/ml granulocyte macrophage colony-stimulating factor (GM-CSF) (Peprotech) for myeloid differentiation; 50 ng/ml fms-related tyrosine kinase 3 ligand (Flt3L) (Peprotech), 50 ng/ml SCF (Kirin), and 10 ng/ml IL-7 (Peprotech) for B- and T-lymphoid differentiation. T-cell induction was induced by coculture with OP9-Dll cells instead of OP9 cells. The differentiated cells were subjected to May-Grünwald Giemsa staining and labeled with biotin-conjugated anti-Mac-1 (BioLegend), PE-conjugated anti-CD19 (BioLegend), biotin-conjugated anti-CD8 (BioLegend), and PE-conjugated anti-CD4 (BioLegend) antibodies. Biotinylated antibodies were visualized with allophycocyanin-conjugated streptavidin (BioLegend).

Gene Expression Analysis and Reporter Assays

RT-PCR was performed as previously described [16]. Briefly, total RNA was isolated using the RNeasy mini kit (QIAGEN, Valencia, CA, http://www.qiagen.com). For RT-PCR, cDNA was synthesized from 500 ng RNA using the PrimeScript reverse transcription kit (Takara, Shiga, Japan, http://www.takara.co.jp) and amplified with Taq DNA polymerase (Takara) according to the manufacturer's recommendations. Primer sequences are listed in Supporting Information Table S1. Real-time PCR was carried out on Light Cycler 480 (Roche Diagnostics, Indianapolis, IN, www.roche.com) according to the manufacturer's instruction. For microarray analysis, total RNA was extracted from *Lhx2*-expressing KSL/KL cells induced from iLhx2-ESCs by the addition of dox (+dox) and these cells were cultured for a further 3 days

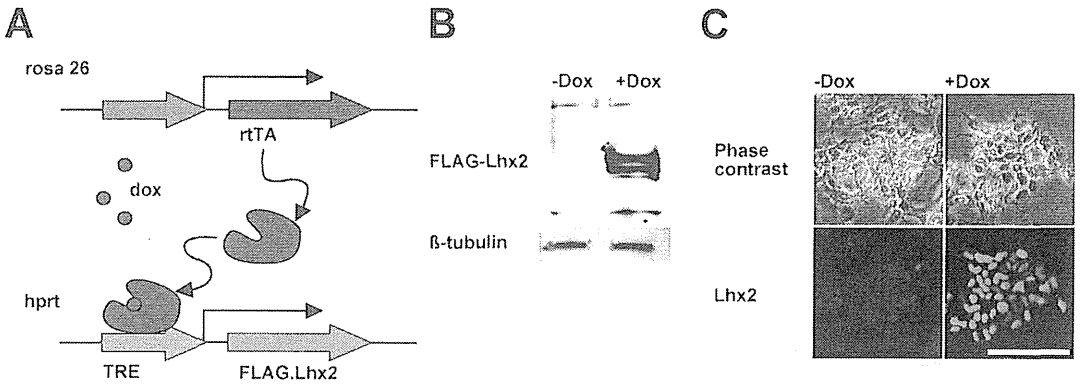

Figure 1. Generation of iLhx2-embryonic stem cells (ESCs). **(A):** The inducible cassette exchange system. Genes of interest can be targeted to a specific conditionally regulated locus. The transactivator *rtTA* and a tetracycline responsive element were introduced at *Rosa26* and *Hprt* loci, respectively. **(B):** iLhx2-ESCs were cultured in the presence or absence of dox for 1 day. Lhx2 expression was detected by Western blotting with an anti-FLAG antibody. **(C):** iLhx2-ESCs were cultured in the presence or absence of dox for 1 day and then stained with an anti-Lhx2 antibody and an Alexa564-conjugated anti-rabbit antibody. Scale bar = 100 μm.

without dox (−dox). The 3D-gene Mouse Oligo chip 24k (Toray, Tokyo, Japan, http://www.toray.com) was used for microarray analysis. RNA was labeled and hybridized to the array chips.

The Lhx2 deletion mutants were synthesized by deleting HD region for Lhx2ΔHD (nucleotides 1–720) and deleting LIM domain for Lhx2ΔLIM (nucleotides 601–1,221). FLAG sequence was inserted into the end of N termini. To construct the LIM domain point mutations, histidine residues (amino acid number 74 and 137, respectively) of N- and C- fingers of the LIM domains of FLAG.Lhx2 were replaced to glycine residues. These Lhx2 mutants were subcloned into pMY-IRES-EGFP retroviral vector.

A genomic fragment around the human *CGA* promoter was cloned from 293T cells and inserted into the pGL3-Basic reporter plasmid (Promega) to generate pGL3-hCGA. pGL3-hCGA was cotransfected with pRL-TK and pMY-Lhx2-IRES-EGFP or its derivatives into 293T cells using the $CaPO_4$ method. Luciferase activity was measured using the dual luciferase reporter assay system (Promega). The transcription efficiency was calculated according to the activity of pRL-TK. The transfection of pGL3-hCGA and pRL-TK into iLhx2-ESCs was carried out by FuGene HD transfection reagent (Promega).

Western Blot Analysis and Immunofluorescent Staining

293T cells were cotransfected with pCMV-Lhx2, pCMV-FLAG-Lmo2, and pCMV-HA-Ldb1 using the $CaPO_4$ method. Western blotting was performed as previously described [20]. Briefly, 2×10^5 cells were collected 2 days after transfection, suspended in 100 μl of SDS-lysis buffer, and sonicated. Twenty microliters of the cell lysate was loaded onto a 10% polyacrylamide gel and transferred onto a polyvinylidene difluoride membrane. The membranes were stained with an HRP-conjugated anti-FLAG antibody (Sigma), a rat anti-HA antibody (Sigma), or a goat anti-Lhx2 antibody (Santa Cruz Biotech, Santa Cruz, CA, www.scbt.com) followed by an HRP-conjugated anti-rat IgG antibody (GE healthcare, Chalfont St. Giles, Buckinghamshire, U.K., http://www.gelifesciences.com), or an HRP-conjugated anti-goat IgG antibody (Abcam, Cambridge, MA, www.abcam.com). A mouse anti-β-tubulin antibody (Sigma) was used as a loading control in combination with an HRP-conjugated anti-mouse IgG antibody (GE healthcare). 293T cells transfected with pCMV-FLAG-Lmo2 and pCMV-HA-Ldb1 with/without pCMV-Lhx2 were treated with 10 μM MG132 (Sigma) for 8 hours. Coimmunoprecipitation assays were carried out as previously described [20]. Quantitative analyses were carried out by LAS3000 imaging system (FUJIFILM, Tokyo, Japan, http://fujifilm.jp).

For immunofluorescent staining of ESCs, a goat anti-Lhx2 antibody was used with Alexa564-conjugated anti-goat IgG antibody (Invitrogen). Fluorescent image was captured using IX71 microscope (Olympus, Tokyo, Japan, http://www.olympus-global.com).

Results

Conditional Expression of Lhx2 During Mouse ESC Differentiation

The dox-mediated gene expression system (inducible cassette exchange) was used to conditionally express *Lhx2* in mouse ESCs (Fig. 1A) [17]. This inducible gene expression system uses Cre/LoxP recombination to introduce a transgene into the host genome. Therefore, clonal variation due to random transgene integration into the host genome is excluded. Using this system, we established a mouse ESC line with inducible *FLAG-Lhx2* expression (iLhx2-ESCs). The expression of FLAG-Lhx2 was dependent on the addition of dox as revealed by Western blotting and immunofluorescent staining using anti-FLAG and anti-Lhx2 antibodies, respectively (Fig. 1B, 1C).

When ESCs were put onto OP9 stromal cells without leukemia inhibitory factor, ESCs were differentiated into mesodermal cells on day 5 of the differentiation induction. We previously showed that retroviral transduction of *Lhx2* into ESC-derived differentiated cells on day 5 results in the accumulation of KSL/KL cells [14]. Therefore, we investigated whether dox-mediated conditional expression of Lhx2 induced the same phenotypes. iLhx2-ESCs were cocultured with OP9 cells for 5 days in the absence of dox. Then, cells were reseeded onto fresh OP9 cells with IL-6 and SCF in the presence or absence of dox. In the absence of dox, approximately 50% of cells differentiated into lineage-positive (Lin^+) cells by day 14 (Fig. 2A). In contrast, almost all cells were lineage-negative (Lin^-) cells in the presence of dox. These cells contained KSL and KL cells. These data are consistent with our previous data using retroviral transduction of *Lhx2* [14].

Accumulation of KSL/KL Cells by Inducible Expression of Lhx2

We next analyzed the time course of KSL/KL cell production after the induction of Lhx2 expression. Lhx2 expression was induced from day 5, and analyzed on days 7 and 9. Most cells were Lin^- on day 5 and in the absence of Lhx2 induction, Lin^+ cells were gradually differentiated by days 7 and 9 (Fig.

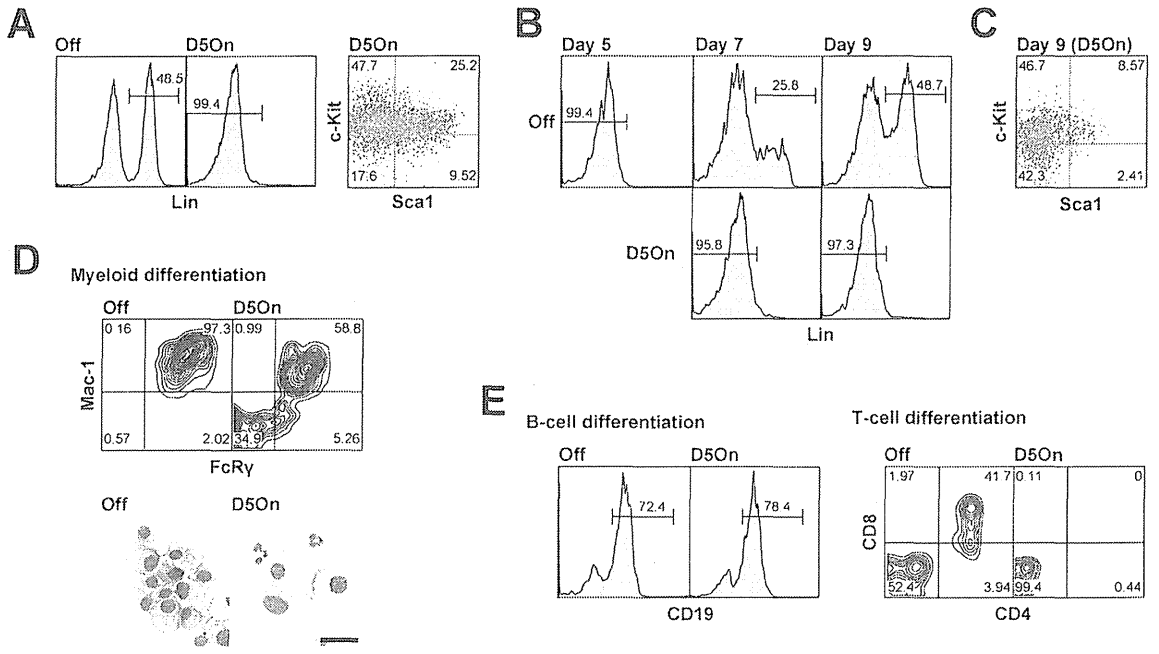

Figure 2. Induction of c-Kit$^+$/Sca1$^+$/lineage$^-$ (KSL)/c-Kit$^+$/Sca1$^-$/lineage$^-$ (KL) cells from iLhx2-embryonic stem cells (ESCs). **(A):** Effects of dox-induced Lhx2 expression on KSL/KL cell formation. iLhx2-ESCs were differentiated on OP9 cells without dox for 5 days, and then cells were recovered and reseeded on OP9 cells with IL-6/SCF in the absence (Off) or presence (D5On) of dox. Fluorescence-activated cell sorting analysis was performed on day 14. **(B):** Lhx2 promotes the accumulation of Lin$^-$ cells. Lhx2 expression was started on day 5 and cells were analyzed on days 7 and 9. **(C):** c-Kit/Sca1 staining of Lhx2-expressing cells on day 9. **(D, E):** Effects of Lhx2 on lineage-directed differentiation. Induction of *Lhx2* was started on day 5 in the presence of granulocyte macrophage colony-stimulating factor on OP9 cells (D), or in the presence of IL-7/SCF/Flt3L on OP9 cells (E, left) or OP9-Dl1 cells (E, right). Scale bar = 50 μm.

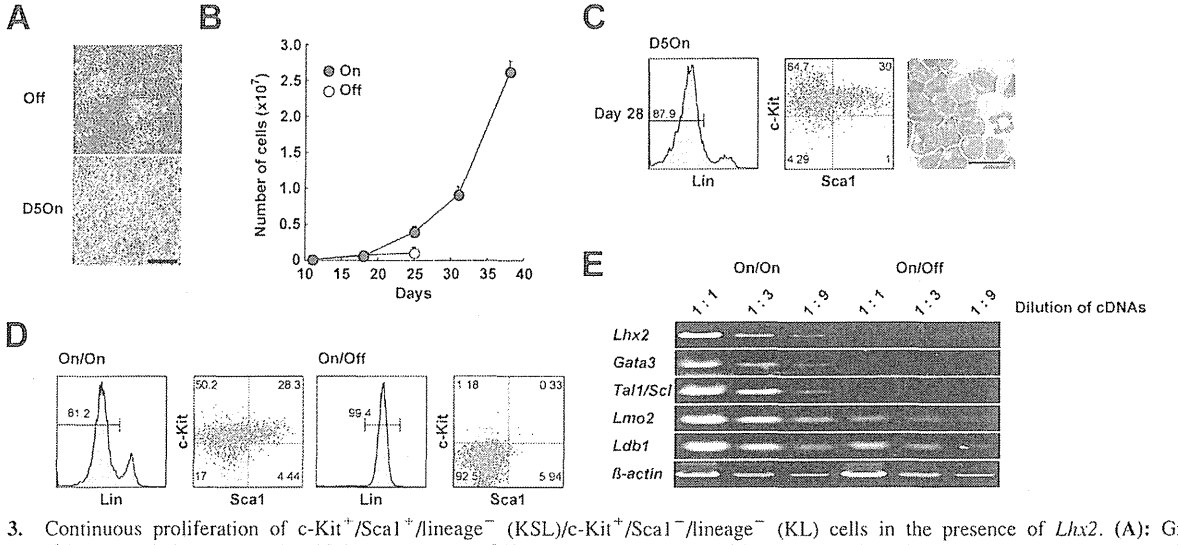

Figure 3. Continuous proliferation of c-Kit$^+$/Sca1$^+$/lineage$^-$ (KSL)/c-Kit$^+$/Sca1$^-$/lineage$^-$ (KL) cells in the presence of *Lhx2*. **(A):** Gross appearance of hematopoietic cells on day 20 in the absence (Off) or presence (D5On) of Lhx2 expression. Expression of Lhx2 was started on day 5. Scale bar = 100 μm. **(B):** Number of hematopoietic cells in the absence or presence of Lhx2. Mean values are plotted ($n = 5$) and the error bars show SDs. **(C):** Lineage/c-Kit/Sca1 and May-Grünwald Giemsa staining of Lhx2-induced cells on day 28. Scale bar = 100 μm. **(D, E):** Effects of Lhx2 withdrawal on KSL/KL cells. Lhx2-induced KSL/KL cells were cultured in the presence (On/On) or absence (On/Off) of Lhx2 from day 28 for 7 days. Fluorescence-activated cell sorting (D) and semiquantitative RT-PCR (E) analyses are shown. cDNAs were serially diluted (1:1, 1:3, and 1:9) and used for semiquantitative RT-PCR.

2B). By contrast, *Lhx2* induction inhibited the lineage differentiation, thereby Lin$^-$ cells accumulated. These Lin$^-$ cells on day 9 contained KSL/KL cells (Fig. 2C). However, we previously reported that *Lhx2*-transduced KSL/KL cells can differentiate into mature hematopoietic cells in vivo and in vitro [14]. Therefore, the effects of dox-induced Lhx2 expression on hematopoietic terminal differentiation were reinvestigated using hematopoietic cytokines. Cytokines were added to the culture medium and Lhx2 expression was induced on day 5. Myeloid cells and B cells were generated when GM-CSF and Flt3L/IL-7/SCF were added, respectively (Fig. 2D, 2E). Thus, Lhx2 did not block cytokine-induced differentiation into myeloid cells and B cells, although the efficiency of myeloid cell differentiation was reduced when Lhx2

Table 1. Transcription factors upregulated by *Lhx2*

Gene	Description	RefSeq_id	Fold increase
Hesx1	Homeobox gene Expressed in ESCs	NM_010420	11.9
Tcf3	Transcription factor 3	NM_009332	9.3
Gata3	GATA binding protein 3	NM_008091	6.4
Sox4	SRY-box containing gene 4	NM_009238	3.9
Ebf2	Early B-cell factor 2	NM_010095	3.6
Tal1	T-cell acute Lymphocytic leukemia 1	NM_011527	3.0
Stat4	Signal transducer and activator of transcription 4	NM_011487	3.6
Stat3	Signal transducer and activator of transcription 3	–	2.9
Hoxa5	Homeobox A5	NM_010453	2.8
Foxo1	Forkhead box O1	NM_019739	2.8
Egr1	Early growth response 1	NM_007913	2.6
Meis1	Myeloid ecotropic viral integration site 1	–	2.6
Hoxd4	Homeobox D4	NM_010469	2.4
Smad1	MAD homolog 1 (Drosophila)	NM_008539	2.3
Evi1	Ecotropic viral integration site 1	NM_007963	2.3
Gfi1b	Growth factor independent 1B	NM_008114	2.3
Hoxd8	Homeobox D8	XM_355338	2.3
Nfya	Nuclear transcription factor-Y alpha	–	2.0

Abbreviation: ESC, embryonic stem cell.

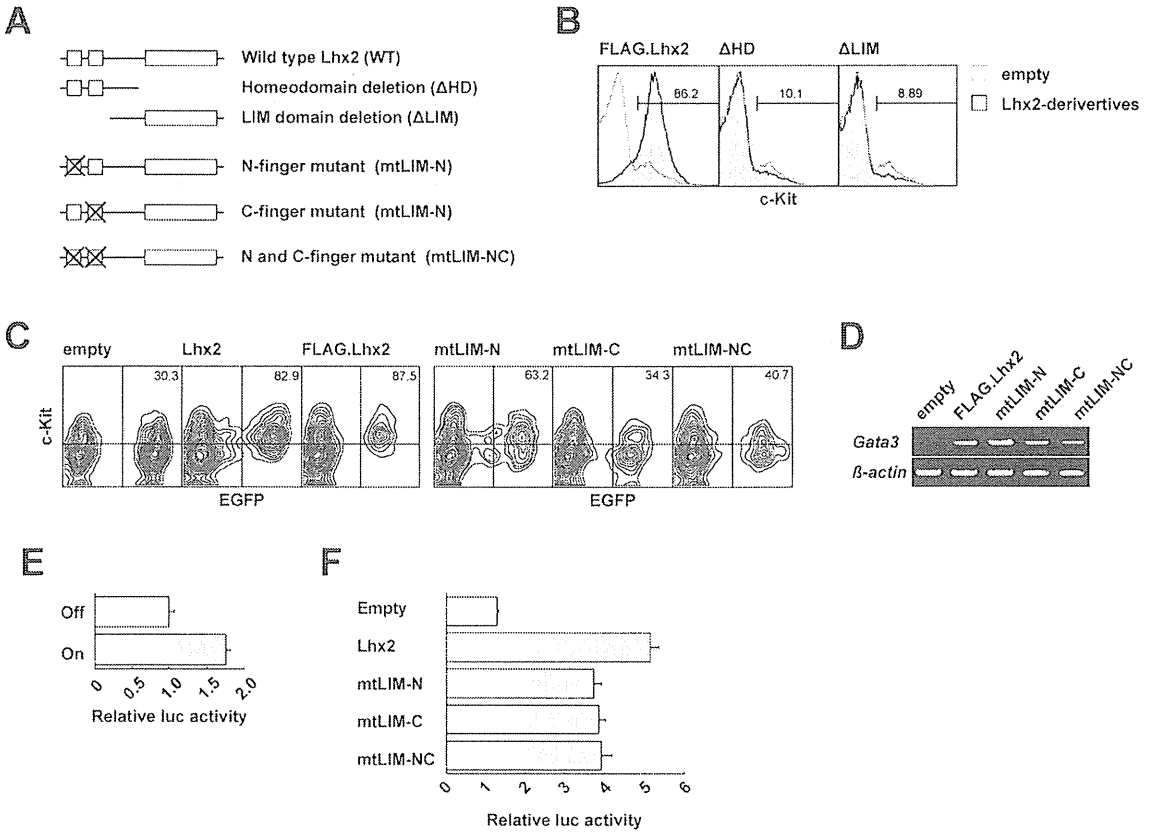

Figure 4. Analysis of Lhx2 mutants. **(A):** Lhx2 mutant constructs. **(B, C):** c-Kit staining of cells transduced with *FLAG-Lhx2* or *Lhx2* mutants. $EGFP^+$ cells are shown (B). E14tg2a embryonic stem cells (ESCs) were differentiated on OP9 cells, and various retroviral vectors harboring *Lhx2* or mutated *Lhx2* were transduced on day 5. The transduced cells were analyzed on day 11. Numbers denote the percentage of $EGFP^+$ cells that were c-Kit^+ (C). **(D):** RT-PCR analysis of *Gata3* expression after transduction of *Lhx2* and *Lhx2* mutants. **(E):** Activation of *hCGA* promoter in ESCs. iLhx2-ESCs were transfected with *hCGA*-luc and pRL-TK and cultured with/without dox. **(F):** Reporter assays of Lhx2 LIM domain point mutants. *Lhx2* or *Lhx2* mutants were cotransfected with the reporter plasmid *hCGA*-luc and pRL-TK into 293T cells. (E, F): Bars show mean values ($n = 5$) and error bars show SD.

expression was induced. Conversely, T-cell induction was severely impaired by Lhx2 in the presence of OP9-Dl1 cells (Fig. 2E), consistent with our previous in vivo data [14]. Thus, Lhx2-induced KSL/KL cells preferentially undergo self-renewal in the presence of IL-6/SCF, but retain multilineage differentiation potentials.

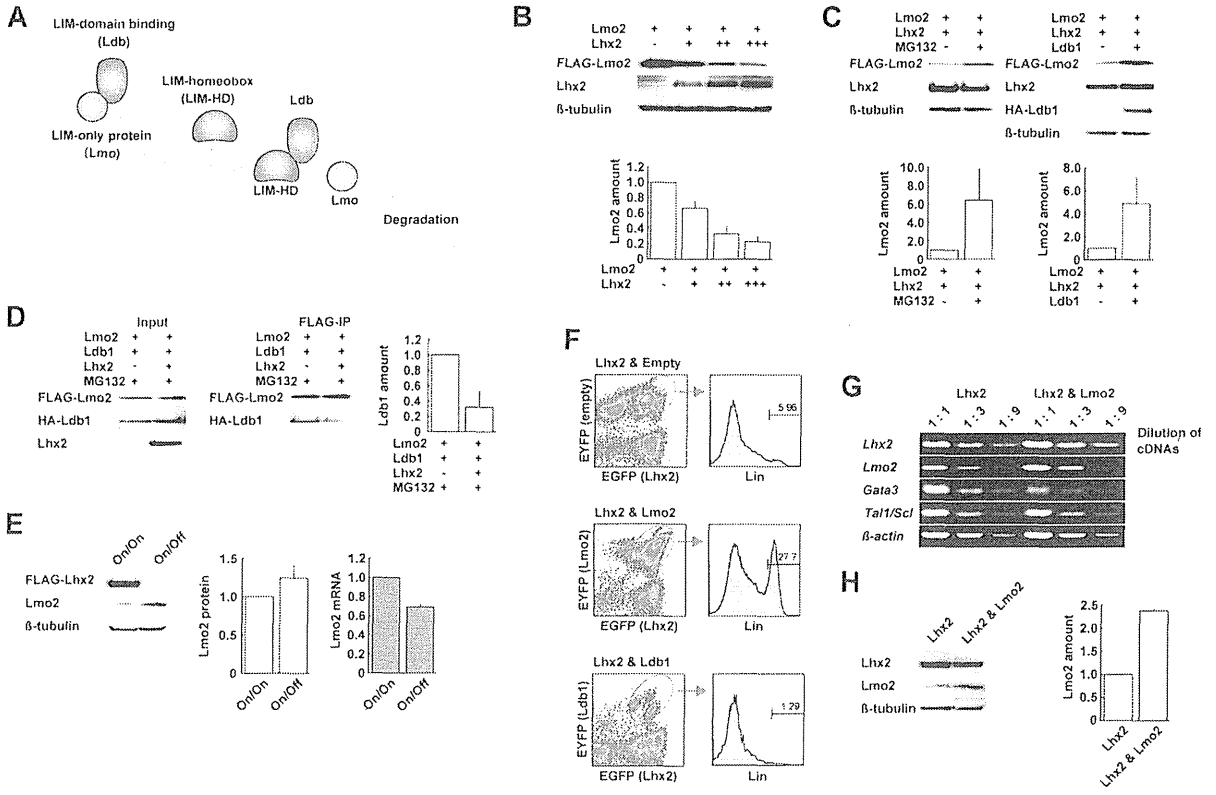

Figure 5. Lhx2 promotes degradation of Lmo2. **(A):** Schematic of the Lmo degradation pathway in the presence of LIM-HD. In the presence of excess LIM-HD, Ldb dissociated from Lmo and the LIM-HD:Ldb complex forms. The dissociated Lmo becomes unstable and is degraded by the E3 ubiquitin ligase Rlim. **(B):** Effects of Lhx2 on the level of Lmo2. FLAG-Lmo2 expression vector (4 μg) was cotransduced with 0 (−), 1 (+), 2 (++), and 4 μg (+++) of Lhx2 expression vector into 293T cells. **(C):** Effects of MG132 and Ldb1 on Lhx2-induced decrease of Lmo2. **(D):** Coimmunoprecipitation assay. Lmo2 and Ldb1 were cotransfected into 293T cells with/without Lhx2. These cells were cultured in MG132 and Lmo2 complex was immunoprecipitated by anti-FLAG antibody and the amount of Ldb1 was analyzed. **(E):** Effects of Lhx2 withdrawal on the level of endogenous Lmo2 in induced KSL/KL cells. Lhx2-induced KSL/KL cells were cultured in the presence (On/On) or absence (On/Off) of Lhx2 for 3 days, and the level of Lmo2 protein and mRNA was analyzed by Western blotting and real-time PCR, respectively. **(F):** Effects of *Lmo2* on KSL/KL cell accumulation. Empty, *Lmo2* and *Ldb1* vectors harboring EYFP were cotransduced with the *Lhx2* vector harboring EGFP on day 5 of differentiation induction of embryonic stem cells and analyzed on day 19. Lineage staining of the $EGFP^+/EYFP^+$ cell fraction was shown. **(G):** Effects of *Lmo2* cotransduction on gene expression. cDNAs were serially diluted (1:1, 1:3, and 1:9) and analyzed by semiquantitative RT-PCR. **(H):** The protein expression of Lhx2 and Lmo2 in Lhx2/Lmo2 cotransduced cells. (B-E, H): Quantified analyzes were shown as bars. Error bars indicated SD ($n = 3$). (B, C, E, H): The amount of Lmo2 protein was normalized by β-tubulin. (D): The amount of immunoprecipitated Ldb1 was normalized by input Ldb1. (E): Lmo2 mRNA expression was normalized by β-actin mRNA. Abbreviation: LIM-HD, LIM-homeobox domain.

Lhx2-induced hematopoietic cells expanded well on OP9 stromal cells by day 20 (Fig. 3A), and the number of hematopoietic cells continued to increase throughout the time course (Fig. 3B). On day 28, KSL and KL cells were still present and were morphologically blastic (Fig. 3C). We next examined whether continuous expression of Lhx2 is required to maintain induced KSL/KL cells. Lhx2-induced KSL/KL cells were cultured with or without dox for 7 more days. In the presence of dox, most cells were KSL or KL (Fig. 3D). By contrast, all cells were Lin^+ in the absence of Lhx2 (Fig. 3D). Thus, continuous expression of Lhx2 is required for the expansion of KSL/KL cells. Lhx2 expression was hardly detected in the absence of dox (Fig. 3E).

Identification of Lhx2-Target Genes

Microarray analysis was performed to identify candidate genes that are regulated by Lhx2. Lhx2-induced KSL/KL cells (+dox) were cultured in the absence of Lhx2 expression for 3 days (−dox), and the gene expression profiles of these two groups of cells were compared (accession number: GSE44778). In the presence of Lhx2, 954 genes were upregulated (more than twofold) and 1,311 genes were downregulated (less than twofold). The top 50 genes that Lhx2 upregulated and downregulated are shown in Supporting Information Table S2A, S2B, respectively. Several HSC marker genes were upregulated by Lhx2 (Supporting Information Table S2C). Of note, components of Gata transcription factor complexes (*Gata3* and *Tal1/Scl*) and Hox transcription factors (*HoxA5*, *HoxD4*, and *HoxD8*) were upregulated by Lhx2 (Table 1). The downregulated genes were mainly differentiation-associated genes (Supporting Information Table S2B). Another ESC line with inducible Lhx2 expression was previously established and candidate *Lhx2* target genes in HPCs were investigated by microarray analysis [21]. In this case [21], ESC-derived HPCs induced by Lhx2 were analyzed at 36, 72, and 96 hours after dox removal. According to the report, 170 genes were upregulated in the presence of Lhx2. When we compared it with our data, 26 genes were commonly upregulated by Lhx2 (Supporting Information Fig. S1).

Molecular Mechanisms Underlying Lhx2-Induced Expansion of HSC-Like Cells

To elucidate the molecular function of Lhx2, we made deletion mutants (Fig. 4A) lacking various regions of Lhx2 and

introduced each mutant into differentiating ESCs by retrovirus-mediated gene transfer. Lhx2 mutant lacking the HD (ΔHD) or LIM (ΔLIM) domain did not amplify c-Kit$^+$ cells (Fig. 4B), indicating that both domains are required for the expansion of KSL/KL cells. Next, we evaluated point mutants of the LIM domain. The N-finger mutant (mtLIM-N) marginally reduced c-Kit$^+$ cell expansion, whereas the C-finger mutant (mtLIM-C) and the double mutant (mtLIM-NC) markedly reduced c-Kit$^+$ cell expansion (Fig. 4C). The expression levels of *Gata3*, a candidate Lhx2 target gene identified by our microarray analysis, were positively correlated with the frequency of c-Kit$^+$ cells in HPCs transduced with these Lhx2 mutants (Fig. 4D). However, it remains determined whether or not Lhx2 directly upregulates *Gata3* mRNA via direct transcriptional activation.

To examine the capacity of each Lhx2 mutant as a transcriptional activator, we used the human *CGA* promoter that is used for monitoring the transcription-enhancing activity of LIM-HD transcription factors [22]. The reporter activity was significantly increased by dox addition in iLhx2-ESCs (Fig. 4E), verifying that the human *CGA* promoter works in mouse ESCs. Subsequent reporter assays revealed that mtLIM-N, mtLIM-C, and mtLIM-NC possessed similar transcription-enhancing activities (Fig. 4F). These data suggest that the expansion of c-Kit$^+$ cells and the transcription-enhancing capacity of Lhx2 are not associated with each other. Therefore, we sought to identify a function of Lhx2 that is independent of the transcriptional regulation.

Degradation of Lmo2 in the Presence of Lhx2

It has been reported that LIM-HD proteins affect the stability of Lmo proteins (Fig. 5A) [23]. Therefore, we investigated the status of hematopoietic Lmo protein, Lmo2. *FLAG-Lmo2* was cotransfected with increasing amounts of *Lhx2* into 293T cells, and the amount of FLAG-Lmo2 was quantified by Western blotting. Quantity of FLAG-Lmo2 protein was gradually decreased when the amount of Lhx2 was increased (Fig. 5B). Addition of the proteasome inhibitor MG132 inhibited this Lhx2-induced reduction of Lmo2 protein expression (Fig. 5C), suggesting that it is a ubiquitin/proteasome-dependent protein degradation. Next, the reduction of Lmo2 protein expression in the Lhx2-transfected cells was rescued by cotransfection of *Ldb1* expression vector (Fig. 5C). Differences in the amount of Lmo2 protein in each experiment were statistically significant ($p < .05$ by Student's t test) when normalized with the levels of β-tubulin. These data indicated that Lhx2 disrupts the Lmo2:Ldb1 complex and released Lmo2 became unstable. Presumably, overexpression of Ldb1 blocks Lmo2 degradation by promoting the Lmo2:Ldb1 complex formation, as shown in a previous study [23]. To confirm this possibility, we carried out coimmunoprecipitation assays in the presence of MG132 to prevent Lmo2 degradation. When FLAG-Lmo2 and HA-Ldb1 were cotransfected, HA-Ldb1 was successfully recovered in the anti-FLAG (Lmo2) immunoprecipitate (Fig. 5D). In the presence of Lhx2, the amount of HA-Ldb1 bound to FLAG-Lmo2 was decreased to approximately one-third of all (Fig. 5D).

Next, we examined endogenous Lmo2 protein levels in the ESCs. KSL/KL cells were generated from iLhx2-ESCs by dox addition and subcultured in the absence or presence of dox for 3 days. Lower amount of Lmo2 protein was detected in the continuous presence of dox when compared with the cells without dox in the last 3 days (Fig. 5E), again demonstrating the destructive action of Lhx2 against Lmo2 protein. Conversely, *Lmo2* mRNA was moderately reduced (approximately 0.7-fold) in the absence of Lhx2 based on real-time PCR analysis (Fig. 5E). This could be a negative feed-back regulation.

To clarify whether the level of Lmo2 affects the *Lhx2*-induced generation of KSL/KL cells, we investigated the effect of Lmo2 overexpression. ESC-derived mesodermal cells were coinfected with empty, Lmo2, or Ldb1 retroviral vectors harboring IRES-EYFP in combination with Lhx2-IRES-EGFP. Expression of Lhx2 and Lmo2 was monitored by EGFP and EYFP fluorescence, respectively. When *Lhx2* and *Lmo2* were cotransduced, the proportion of Lin$^+$ cells in the EGFP$^+$/EYFP$^+$ cell fraction increased (Fig. 5F). Conversely, EGFP$^+$/EYFP$^-$ cells, namely Lhx2$^+$/Lmo2$^-$ cells, were mostly KSL/KL cells in all three samples (Supporting Information Fig. S2A). Cotransduction of *Ldb1* slightly increased the proportion of Lin$^-$ cells (Fig. 5F). This might be due to the enhancement of Lhx2 activity by Ldb1, since Lhx2 and Ldb1 work together. Thus, the level of Lmo2 is crucial for the Lhx2-induced expansion of KSL/KL cells. To clarify whether Lmo2 affects the initial emergence of KSL/KL cells, or whether Lmo2 disrupts the self-renewal of KSL/KL cells, *Lmo2* was introduced into cells after transduction of *Lhx2*. *Lhx2* was first introduced on day 5 and *Lmo2* was subsequently transduced on day 9 or 12. The proportion of Lin$^+$ cells still increased in both cases (Supporting Information Fig. S2B), although percentage of the Lin$^+$ population steeply decreased when *Lmo2* was transduced on day 12. These data suggest that Lmo2 inhibits the Lhx2-mediated expansion of KSL/KL cells when present in an early-stage of the population establishment. The Lin$^+$ cells generated by cotransduction of *Lhx2* and *Lmo2* were mainly Mac-1$^+$ (Supporting Information Fig. S2C).

Inhibition of Mature Hematopoietic Cell Differentiation by Gata3

Microarray analysis revealed that *Gata3* and *Tal1/Scl* mRNAs were upregulated by Lhx2 overexpression. These data were confirmed by semiquantitative RT-PCR (Fig. 3E). Gata3 is expressed in adult HSCs and in the aorta/gonad/mesonephros regions in which HSCs emerge [15, 24]. Tal1/Scl is an interaction partner of Lmo2, and is required for the HSC development in mouse embryos [25, 26]. Therefore, we focused on these molecules. When *Lmo2* and *Lhx2* were cotransduced, the expression of *Gata3* but not *Tal1/Scl* was reduced (Fig. 5G). We confirmed the increase of Lmo2 protein in these experiments (Fig. 5H). Thus, Gata3 expression may be more related to the Lhx2-induced expansion of KSL/KL cells. We newly generated an ESC line carrying an inducible Gata3 expression cassette (iGata3-ESCs) and investigated the effects of Gata3 overexpression. When Gata3 was expressed from day 5, hematopoietic cell differentiation was accelerated (Fig. 6A). Induction of Gata3 expression resulted in the accumulation of Lin$^-$ cells (Fig. 6B). However, only a small number of KSL/KL cells were generated in this case. These data indicate that overexpression of Gata3 inhibits the hematopoietic differentiation (Lin$^-$ to Lin$^+$), but is not sufficient for the expansion of KSL/KL cells. Next, we performed *Gata3*-knockdown experiments using a specific shRNA (Supporting Information Fig. S3A). First, lentiviral vectors carrying EGFP in combination with Gata3 shRNA or control shRNA (Supporting Information Fig. S3B) were transduced into iGata3-ESCs and *Gata3* expression was induced by dox. *Gata3* expression was decreased by Gata3 shRNA, but not by control shRNA (Supporting Information Fig. S3C). Next, KSL/KL cells generated from iLhx2-ESCs were infected with these lentiviral vectors. After the transduction, numbers of empty vector- and control shRNA transduced EGFP$^+$ cells were

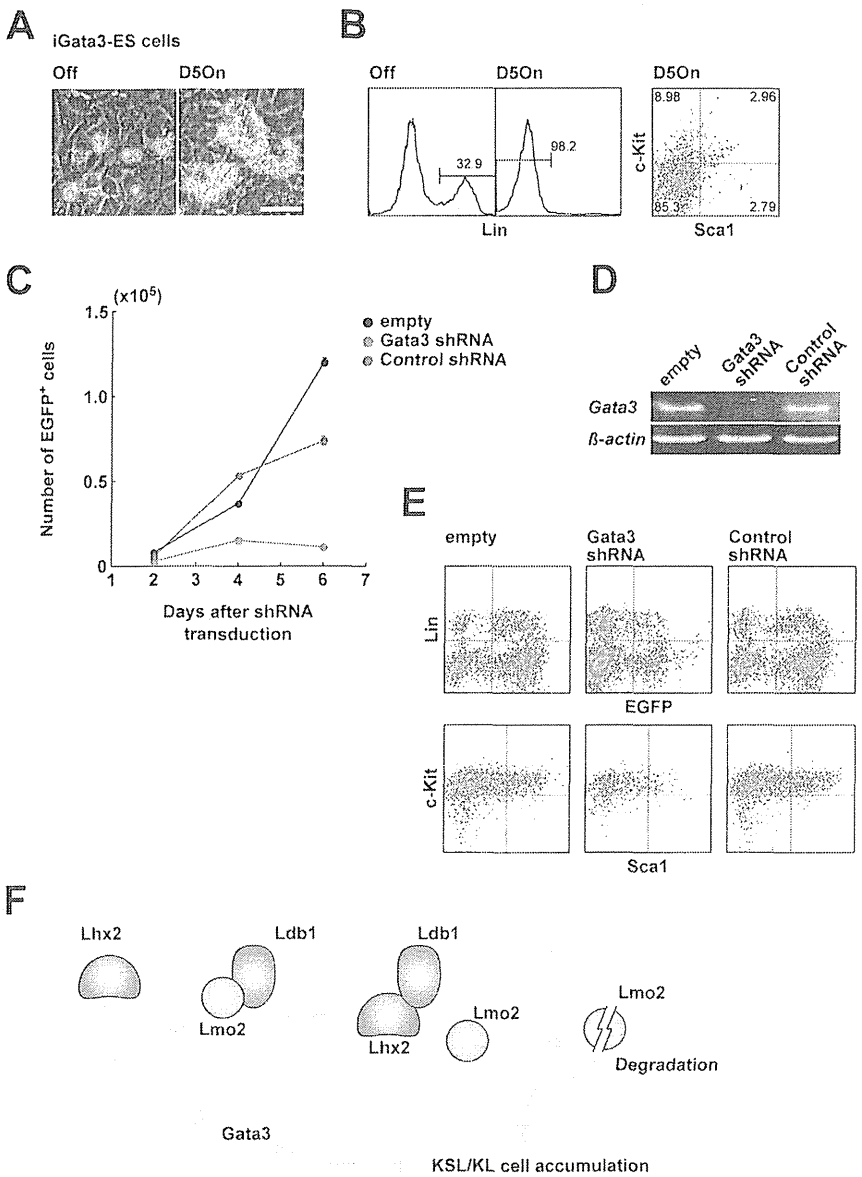

Figure 6. Gata3 function on Lhx2-induced KSL/KL cells. **(A):** Gross morphology of immature hematopoietic colonies on day 7. iGata3-ESCs were differentiated and Gata3 expression was started on day 5. Scale bar = 50 μm. **(B):** Inhibition of Lin^+ cell differentiation on day 13 by Gata3 expression. **(C):** Cell number of Gata3 shRNA-transduced KSL/KL cells induced by Lhx2. Lentiviral vectors carrying EGFP and Gata3 shRNA or control shRNA were transduced into the Lhx2-induced KSL/KL cells. Dots show mean values ($n = 5$) and error bars show SD. **(D):** RT-PCR analysis of *Gata3* expression in shRNA-transduced cells. **(E):** Decrease of KSL cells by Gata3 shRNA. **(F):** Schematic illustration of the proposed molecular functions of Lhx2 in the Lhx2-mediated expansion of ES-derived KSL/KL cells. Abbreviation: ESC, embryonic stem cell.

increased (Fig. 6C). In contrast, Gata3 shRNA-transduced cells were poorly proliferated (Fig. 6C). We confirmed that *Gata3* mRNA was suppressed by Gata3 shRNA but not by control shRNA (Fig. 6D). In addition, generation of KSL/KL cells in $EGFP^+$ cells was inhibited by Gata3 shRNA, but not by control shRNA (Fig. 6E). Thus, Gata3 is required for self-renewal of the Lhx2-induced KSL/KL cells.

Discussion

We previously showed that when *Lhx2* is introduced into mesodermal cells derived from mouse ESCs/iPS cells, HSC-like cells are robustly expanded [14]. These HSC-like cells acquire in vitro self-renewal ability in the presence of IL-6/SCF and OP9 cells without losing their multipotential differentiation ability. In this study, we focused on the role of Lhx2 in the self-renewal of KSL/KL cells. Here, we revealed that Lhx2 inhibits the hematopoietic differentiation of Lin^- cells into Lin^+ cells, and this activity is tightly associated with the expansion of KSL/KL cells. This inhibition of hematopoietic differentiation was in part caused by a decrease in the level of Lmo2 protein, which may occur after disruption of the Lmo2:Ldb1 complex by Lhx2 overexpression (Fig. 6F).

In the presence of a higher amount of Lhx2, several transcription factors were upregulated in ES-derived KSL/KL cells. Among them, Gata3 was involved in the inhibition of hematopoietic differentiation. It remains unknown whether the